MASTERARBEIT | MASTER'S THESIS

Titel | Title

Investigation of the Influence of a Phospholipase A2 from the Venom of the Mexican West-Coast Rattlesnake (Crotalus basiliscus) on Human Blood Coagulation Using a Thrombin Generation Assay

verfasst von | submitted by

Anna Grösslinger BSc

angestrebter akademischer Grad | in partial fulfilment of the requirements for the degree of

Magistra pharmaciae (Mag. pharm.)

Wien | Vienna, 2025

Studienkennzahl lt. Studienblatt | Degree programme code as it appears on the student record sheet:	UA 066 605
Studienrichtung lt. Studienblatt | Degree programme as it appears on the student record sheet:	Masterstudium Pharmazie
Betreut von | Supervisor:	Univ.-Doz. Mag. Dr. Peter Turecek

1 Abstract

This thesis examines the effect of proteins from the Crotalus basiliscus venom on human blood coagulation: a basic phospholipase A2 (PLA2) and proteases that inhibit the alpha-2 macroglobulin (a2M). In general, PLA2s are known for their anticoagulant activity. The underlying mechanism is either hydrolysis of phospholipids or binding to blood coagulation factors. (Saikia & Mukherjee, 2017) This study aims to explore the mechanism of PLA2 in the function of the venom. a2M is a plasma protein, which inhibits a wide range of proteases, including thrombin. When inhibiting thrombin, thrombin can still cleave small peptide substrates. This is a problem of the thrombin generation assay (TGA), because the free thrombin curve is not identical to the amidolytic activity curve, which impacts the area under the curve, which is an important quantitative readout of TGA. Several factors influence the a2M serum concentration, including age, sex, and several pathologies, making a mathematical correction of the curve based on the mean a2M concentration difficult. Use of a2M-inhibiting proteases was suggested as a potential solution to reduce or completely diminish the residual amidolytic activity of the a2M-thrombin complex. (Rijkers et al., 1998; Svoboda et al., 1995)

The proteins were purified using size-exclusion and anion-exchange chromatography, and their effect on blood coagulation was investigated with the TGA. Furthermore, the PLA2 activity was measured using an assay based on the hydrolytic activity of PLA2s towards phospholipids, and the a2M inhibiting activity was evaluated with a plasmin inhibitor assay. Additionally, four substances (Varespladib, Nifedipine, Nisoldipine, and Quinacrine) were chosen to inhibit the PLA2 activity.

The a2M inhibiting proteases showed activity in the plasmin inhibitor assay, but inhibited thrombin generation when added to the plasma for the TGA. After the purification steps, the fractions were not entirely pure, and impurities with a molecular weight of approximately 10 kDa were found, suggesting the presence of PLA2s. The PLA2 inhibited thrombin generation in a time- and phospholipid-dependent manner. The anticoagulant effect was enhanced by increasing the incubation time of the PLA2.

Raising the phospholipid concentration in the TGA reagent decreased the inhibitory effect on thrombin generation. Varespladib inhibited the anticoagulant impact of PLA2 in the TGA, and Nisoldipine only had a minor effect. Nifedipine and Quinacrine inhibited the PLA2 activity in the activity assay but not in the TGA.

From these findings, it can be concluded that Crotalus basiliscus venom contains basic and anticoagulant PLA2 and a2M-inhibiting proteases. Varespladib can significantly inhibit PLA2 activity. These effects can all be measured using the TGA. The potential use of the a2M-inhibiting proteases could not be assessed due to an anticoagulant effect possibly caused by the impurities.

2 Zusammenfassung

Diese Masterarbeit untersucht den Effekt von Proteinen aus dem Gift der Crotalus basiliscus auf die menschliche Blutgerinnung: eine basische Phospholipase A2 (PLA2) und Proteasen, die alpha-2 Makroglobulin (a2M) inhibieren. Im Allgemeinen sind PLA2s für ihre gerinnungshemmende Aktivität bekannt. Der zugrundeliegende Mechanismus basiert einerseits auf der Hydrolyse von Phospholipiden und andererseits auf der Bindung von Blutgerinnungsfaktoren. (Saikia & Mukherjee, 2017) Im Rahmen dieser Arbeit sollen der Mechanismus der PLA2 und ihre Rolle in der Funktion des Giftes untersucht werden. a2M ist ein Plasmaprotein, das ein breites Spektrum an Proteasen inhibiert, einschließlich Thrombin. Trotz der Inhibition bleibt Thrombin jedoch in der Lage, kleine Peptidsubstrate zu spalten. Dies stellt ein Problem für den Thrombin-Generierungs-Assay (TGA) dar, da sich die Kurve des freien Thrombins von der Kurve der amidolytischen Aktivität unterscheidet, was wiederum die quantitative Bestimmung der Fläche unter der Kurve, ein wichtiger Parameter im TGA, erschwert. Die Serumkonzentration von a2M wird von verschiedenen Faktoren beeinflusst, darunter Alter, Geschlecht und verschiedene Erkrankungen, was eine mathematische Korrektur der Kurven zusätzlich erschwert. Der Einsatz von a2M-hemmenden Proteasen wurde als potenzielle Lösung vorgeschlagen, um die amidolytische Restaktivität des a2M-Thrombin-Komplexes zu reduzieren oder gänzlich zu unterdrücken. (Rijkers et al., 1998; Svoboda et al., 1995)

Die Proteine wurden mittels Größenausschluss- und Anionenaustauschchromatographie aufgetrennt und deren Effekt auf die Blutgerinnung mittels TGA untersucht. Zudem wurde die PLA2-Aktivität mithilfe eines Assays quantifiziert, der auf der hydrolytischen Spaltung von Phospholipiden basiert. Die a2M-Aktivität wurde durch einen Plasmin-Inhibitor-Assay bestimmt. Vier Substanzen (Varespladib, Nifedipin, Quinacrine und Nisoldipin) wurden ausgewählt, um die PLA2-Aktivität zu inhibieren.

Die a2M-inhibierenden Proteasen zeigten eine Aktivität im Plasmin-Inhibitor-Assay, führten jedoch nach Zugabe zu Plasma für den TGA zu einer Hemmung der Thrombinbildung. Trotz einer Aufreinigung in zwei Schritten konnten in den Fraktionen Verunreinigungen mit einem Molekulargewicht von etwa 10 kDa nachgewiesen werden. Dies deutet auf PLA2 hin. Die PLA2 hemmte die Thrombin-Generierung in zeit- und phospholipidabhängiger Weise. Der gerinnungshemmende Effekt vergrößerte sich bei verlängerter Inkubationszeit und verringerte sich bei Erhöhung der Phospholipidkonzentration. Varespladib hemmte den gerinnungshemmenden Effekt der PLA2 im TGA und Nisoldipin hatte einen geringen Effekt darauf. Nifedipin und Quinacrine hemmten die PLA2-Aktivität im PLA2-Assay, jedoch nicht im TGA.

Die Ergebnisse lassen darauf schließen, dass das Gift des Crotalus basiliscus eine basische und gerinnungshemmende PLA2 und a2M-inhibierende Proteasen enthält. Varespladib hemmt die PLA2-Aktivität signifikant. Diese Effekte lassen sich mithilfe des TGA nachweisen. Der potenzielle Nutzen der a2M-inhibierenden Proteasen konnte aufgrund gerinnungshemmender Effekte, die vermutlich durch Verunreinigungen verursacht wurden, nicht beurteilt werden.

3 Acknowledgements

First and foremost, I want to thank my supervisor, Univ.-Doz. Prof. Dr. Peter L. Turecek (Department of Pharmaceutical Sciences, University of Vienna), for his expertise and continuous guidance. His commitment to academic excellence and attention to detail have not only shaped the quality of this master's thesis but also profoundly influenced my academic and professional development.

My appreciation also goes to Dr. Nikolaus Binder, PhD, for generously allowing me to conduct the experimental part of my research in his laboratory at Technoclone. His guidance, encouragement, and expertise were invaluable throughout the experimental phase of this research. I am also grateful for the trust he placed in me by allowing me to work independently while also being available for guidance.

I also wish to thank the entire Technoclone Research and Development Department for their generous support and technical assistance and for providing access to the facilities and equipment necessary for this study. Their expertise and collaboration were essential to completing the experimental work.

I am also grateful to my colleagues at Technoclone for their cooperation, encouragement, and the pleasant working atmosphere during my time in the laboratory.

Finally, I would like to express my deepest gratitude to my friends and family, who provided distractions and encouragement whenever needed throughout this entire time and during my studies as well. Their support and companionship helped sustain my motivation during challenging times. I also wish to thank my peers at the university for their insightful discussions, which enriched my research experience and made this journey more meaningful.

4 Table of Contents

5 Abbreviations

a2AP	Alpha-2 Antiplasmin	SEC	Size-exclusion chromatography
a2M	Alpha-2 Macroglobulin	sPLA2	Secreted PLA2
AEC	Anion-exchange chromatography	SVMP	Snake Venom Metalloproteinase
AMC	7-Amino-4-methylcoumarin	svPLA2	Snake Venom Phospholipase A2
FVIII	Coagulation factor VIII	SVSP	Snake Venom Serine Proteinases
HPLC	High performance liquid chromatography	TF	Tissue factor
LD50	Median Lethal dose	TGA	Thrombin Generation Assay
LPLC	Low pressure liquid chromatography	tLag	Lag time
NIF	Nifedipine	tPeak	Time to Peak
NIS	Nisoldipine	VAR	Varespladib
PBS	Phosphate-buffered saline		
PL	Phospholipids		
PLA2	Phospholipase A2		
QUI	Quinacrine		
RFU	Raw optical signal		
SDS-PAGE	Sodium Dodecyl Sulfate-Polyacrylamide Gel electrophoresis		

6 Introduction

6.1 Phospholipase A2

PLA2s are esterases that target the sn-2 position of glycerophospholipids, hydrolyzing the ester bond to release a lysophospholipid and a free fatty acid. They can compromise the integrity of the cell membrane, leading to cell death due to the influx of extracellular molecules. The PLA2 superfamily includes four categories: Ca^{2+}-dependent secreted, Ca^{2+}-dependent cytosolic, Ca^{2+}-independent, and lipoprotein-associated PLA2s. All PLA2 enzymes found in snake venoms belong to the secreted category. The svPLA2 consists of 120-135 amino acids, 6-8 disulfide bridges, and has a molecular weight of 14-18 kDa. svPLA2s are divided into three groups based on their disulfide bonding patterns, amino acid sequences, molecular weight, and loop insertion. PLA2s in the Elapidae family are classified as group IA, those in the Viperidae family as group IIA, and svPLA2s in rear-fanged snakes as group IIE. (Castro-Amorim et al., 2023)

Group IA PLA2s can hydrolyze zwitterionic PL due to aromatic residues on the binding surface, while group IIA PLA2s have basic residues on the surface, making them selective for anionic vesicles. Additionally, svPLA2s in group IIA can bind to factor Xa and inhibit prothrombinase activity; this anticoagulant effect is independent of PL hydrolysis. (Dennis et al., 2011)

The PLA2 molecule has several pharmacological sites: the catalytic site, the neurotoxic site (hydrophobic region around residues 80-110), the myotoxic site (cationic site around residues 79-87), and the anticoagulant site (residues 54-77). (Kini & Evans, 1987; Kini & Iwanaga, 1986; Manjunatha Kini & Iwanaga, 1986)

6.1.1 Crotoxin

Crotoxin, derived from the venom of the South American rattlesnake (Crotalus durissus), is a protein complex with neurotoxic and anticoagulant properties. The composition includes two primary components: Crotoxin B, a basic, enzymatically active Asp49 PLA2, and Crotoxin A, an acidic non-enzymatic domain. The Crotoxin B domain and the Crotoxin complex inhibit the prothrombinase complex formation by interacting with factor Xa. Crotoxin A is also considered an anticoagulant molecule with a lower potency, and it does not bind to factor Xa or inhibit the prothrombinase activity. (Faure et al., 2007; Gimenez et al., 2020)

When added to plasma, it prolongs clotting times in prothrombin time and activated partial thromboplastin time assays, indicating a strong anticoagulant effect acting on different pathway components. Crotoxin impacts prothrombin activity through PL, either by hydrolysis or by competing with coagulation factors for the binding of PL. (Gimenez et al., 2020)

6.1.2 Effect on Blood Coagulation

svPLA2s can be classified into three categories depending on their impact on blood coagulation: potent anticoagulants (at 2 µg/ml), weak anticoagulants (3-10 µg/ml), and non-anticoagulants (above 15 µg/ml). (Kini, 2005) Strong anticoagulant PLA2s are characterized by having basic residues at the anticoagulant site (residues 54 – 77), especially 4 lysine residues. In general, basic PLA2s are more toxic. However, the location of the basic residues is more critical than the basicity of the whole enzyme (pI>9), as not all basic PLA2s are strong anticoagulants. The cationic site is likely necessary to interact with the negatively charged PL. Weak or non-anticoagulant PLA2s have acidic residues in that specific region.(Kini & Evans, 1987; Verheij et al., 1980) His48 is crucial for hydrolysis of PL and is conserved in all svPLA2s. (Kini, 2005)

One mechanism by which the PLAs affect coagulation is through the hydrolysis of PL, as these play a crucial role in the formation of coagulation complexes. (Kini, 2005)

Furthermore, PLA2s can bind to PL or blood coagulation factors and inhibit blood coagulation. (Saikia & Mukherjee, 2017)

Strong anticoagulant PLA2s may prevent the formation of the prothrombinase complex (factors Va, Xa, PL, Ca^{2+}) by binding to factor X or Xa and competing for the PL surface with clotting factors. The enzymatic activity does not correlate with the anticoagulant potency in strong anticoagulants, suggesting a nonenzymatic mechanism. (Saikia & Mukherjee, 2017) The basic residues are also essential for the PL-independent inhibition of prothrombinase activity, as acidic or neutral PLA2s cannot inhibit prothrombinase activity without PL. (C. M. Mounier et al., 2001)

Weak anticoagulant PLA2s mainly inhibit blood coagulation by hydrolyzing PL and therefore target the tenase complex more than the prothrombin complex, as it depends more on PL. (C. M. Mounier et al., 2001)

6.1.3 Inhibitors

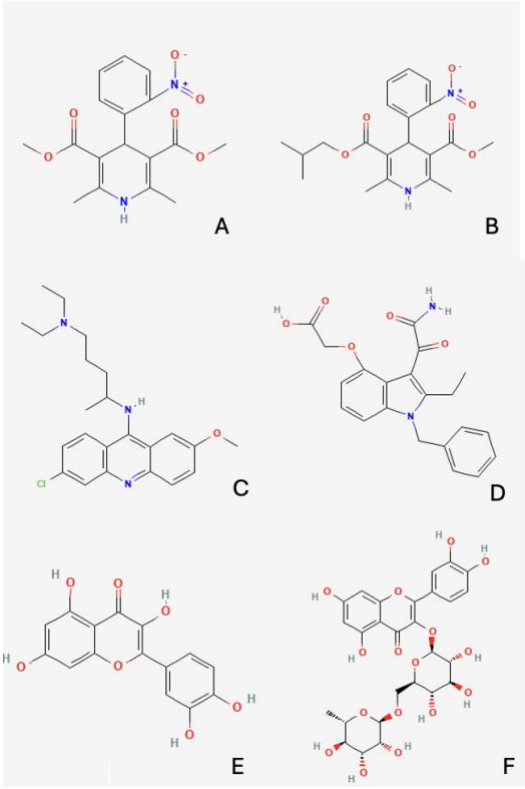

Figure 1. 2D Structures of PLA2 inhibitors. A: NIF, B: NIS, C: QUI, D: VAR, E: Quercetin, F: Rutin; nitrogen in blue, oxygen in red, hydrogen in grey, chloride in neon-green (National Center for Biotechnology Information, 2025f, 2025d, 2025e, 2025a, 2025c, 2025b)

NIF (Figure 1A; IUPAC: dimethyl 2,6-dimethyl-4-(2-nitrophenyl)-1,4-dihydropyridine-3,5-dicarboxylate, $C_{17}H_{18}N_2O_6$) and NIS (Figure 1B; IUPAC: 3-O-methyl 5-O-(2-methylpropyl) 2,6-dimethyl-4-(2-nitrophenyl)-1,4-dihydropyridine-3,5-dicarboxylat,$C_{20}H_{24}N_2O_6$) are 1,4-dihydropyridines substituted by methyl, o-nitrophenyl, and methoxycarbonyl groups. NIF has a second methoxycarbonyl group, while NIS has an isobutoxycarbonyl group at position 5. NIS has a molecular weight of 388,4 g/mol, and NIF has a molecular weight of 346,3 g/mol. (National Center for Biotechnology Information, 2025c, 2025b)

NIF and NIS are drugs used as antihypertensive agents and are classified as calcium antagonists and can inhibit PLA2 activity. The inhibition of PLA2 by NIF and NIS is independent of their calcium-channel blocking activity, as this effect is observable in

cell-free conditions and in the absence of calcium channels. The PLA2 activity can be reduced by more than 90% at a concentration of 100 µM. This effect was only observed with human PLA2; svPLA2s have not been studied yet. (Chang et al., 1987)

QUI (Figure 1C; IUPAC: 4-N-(6-chloro-2-methoxyacridin-9-yl)-1-N,1-N-diethylpentane-1,4-diamine, $C_{23}H_{30}ClN_3O$) is an antimalarial, anthelmintic, and immunomodulatory drug and belongs to the class of acridines substituted by a chloro, a methoxy, and a [5-(diethylamino)pentan-2-yl]nitrilo group. It is also known as mepacrine and has a molecular weight of 400 g/mol. (National Center for Biotechnology Information, 2025a) A potential PLA2-inhibiting activity has been shown in several cell biological experiments for both snake venom PLA2s and human PLA2s. (Çomaklı et al., 2024; Crosland, 1989; Judge et al., 2002; Mustonen et al., 1998; Shimizu et al., 1994)

VAR (Figure 1D; IUPAC: 2-(1-benzyl-2-ethyl-3-oxamoylindol-4-yl)oxyacetic acid, $C_{21}H_{20}N_2O_5$) belongs to the class of indoles; specifically, it is a 1H-indole substituted with benzyl, ethyl, oxamoyl, and carboxymethoxy groups. VAR has a molecular weight of 380,4 g/mol. (National Center for Biotechnology Information, 2025d)

VAR was first developed to treat sPLA2-induced inflammation, which is related to diseases such as rheumatoid arthritis, ulcerative colitis, severe sepsis, and acute coronary and acute chest syndromes. (Salvador et al., 2019). It has also been shown that it can inhibit the effect of PLA2 by reducing the enzymatic, anticoagulant, myotoxic, and cytotoxic effects and prolonging the survival rate of mice when injected with snake venoms. (Gutierres et al., 2022; Kazandjian et al., 2021; Lewin et al., 2016; Salvador et al., 2019) VAR can interact with residues in the hydrophobic channel, e.g., His48 and Lys49, blocking the interaction with fatty acids. (Salvador et al., 2021)

Quercetin (Figure 1E; IUPAC: 2-(3,4-dihydroxyphenyl)-3,5,7-trihydroxychromen-4-one, $C_{15}H_{10}O_7$) is a flavonoid, a pentahydroxyflavone with five hydroxy groups, commonly found in vegetables, fruit, and wine. It has antioxidant, antibacterial, and antineoplastic properties. Rutin (Figure 1F; IUPAC: 2-(3,4-dihydroxyphenyl)-5,7-dihydroxy-3-[(2S,3R,4S,5S,6R)-3,4,5-trihydroxy-6-[[(2R,3R,4R,5R,6S)-3,4,5-trihydroxy-6-methyloxan-2-yl]oxymethyl]oxan-2-yl]oxychromen-4-one, $C_{27}H_{30}O_{16}$) is a rutinoside and the

disaccharide derivative of quercetin with one hydroxy group substituted with rhamnose and glucose sugar groups. The flavonol glycoside can be found in plants such as buckwheat, tobacco, and hydrangea. (National Center for Biotechnology Information, 2025e, 2025f) A PLA2-inhibiting activity has been found for both snake venom and human PLA2s. The molecular weight of Quercetin is 302,2 g/mol, and the molecular weight of Rutin is 610,5 g/mol. (Cotrim et al., 2011; Lindahl & Tagesson, 1997; National Center for Biotechnology Information, 2025e, 2025f)

6.2 Snake Venom Metalloproteinases

SVMPs are enzymes found in snake venoms. They belong to the metalloproteinase family and are zinc-dependent. Depending on their size and domain structure, they can be classified into three classes: the P-I, P-II, and P-III. (Olaoba et al., 2020) (Fox & Serrano, 2008)

SVMPs can consist of four main domains: the prodomain, metalloproteinase, disintegrin, and cysteine-rich domains. The prodomain is mainly responsible for the maturation of SVMPs. The metalloproteinase domain influences the hemorrhagic, fibrinolytic, and apoptotic activity of the toxin. The disintegrin domain is responsible for inhibiting platelet aggregation and cell adhesion, impairing cell migration, and enhancing the metalloproteinase activity. The Cysteine-rich domain also inhibits platelet aggregation and promotes hemorrhage activities. (Olaoba et al., 2020)

The P-I SVMPs have a molecular weight of 20 – 30 kDa and consist of only a metalloproteinase domain. The zinc-binding site can be found in this domain, which is characterized by a conserved sequence (HEXXHXXGXXH) followed by a “methionine-turn” motif. They have proteolytic, hemorrhagic, and edema-forming activities, but are less toxic than P-II and P-III SVMPs. (Olaoba et al., 2020)

Members of the P-I SVMPs have a similar structure, but their hemorrhagic activity can be different. Non-hemorrhagic P-I SVMPs have great flexibility in the loop region near the active site, while hemorrhagic members have greater flexibility in the loop area before the Met-turn. (Camacho et al., 2019)

The P-II SVMPs can have a molecular mass of 30 to 60 kDa and include multiple domains, such as a pro-domain, a metalloproteinase, and a disintegrin domain. Some P-II members can inhibit platelet aggregation due to an integrin-binding motif called the RGD-motif (arginine-glycine-aspartate). (Olaoba et al., 2020)

The P-III class has the most complex structure and the highest molecular mass (60 to 100 kDa). (Olaoba et al., 2020). It contains a metalloproteinase, disintegrin-like, and cysteine-rich domains. Due to the non-catalytic disintegrin-like and cysteine-rich domains, P-III SVMPs have strong hemorrhagic activities. Furthermore, they are resistant to inactivation by a2M, a plasma proteinase inhibitor. (Escalante et al., 2011)

6.3 Crotalus Basiliscus

Figure 2. Crotalus basiliscus (Dollingers, 2025)

Crotalus basiliscus, also called the Mexican west coast rattlesnake, belongs to the family of Viperidae and the genus Crotalus. It is endemic to Mexico and distributed in the following states: Sinaloa, Nayarit, Jalisco, Colima, Michoacan, Sonora, Zacatecas, Aguascalientes, and Chihuahua. (Uetz, n.d.) It can be found in tropical deciduous, thorn, oak forests, as well as subtropical Mimosaceae cacti thorn scrub vegetation types. It is not endangered but has a high environmental vulnerability score and is subject to special protection according to the SEMARNAT (Secretaría de Medio Ambiente y Recursos Naturales) (Lemos-Espinal & Smith, 2020). It can reach a snout-vent length of 150-204 cm, making it the largest rattlesnake in Mexico. (Segura et al., 2017) 24 to 41 diamond-shaped body blotches can be found on the snake, which have a

yellow or yellowish white outline. The ground color can be pale brown, yellowish olive, olive-gray, or greenish olive. The rattle matrix is typically grey or brown. (McCranie, 1981) The coloring can be seen in Figure 2.

6.3.1 Epidemiological Data

To date, limited scientific research has been conducted on the venom of Crotalus basiliscus. This lack of research may be due to the low incidence of envenomation cases in the endemic regions of Crotalus basiliscus. (Méndez-Molina et al., 2024) This might be because the states where Crotalus basiliscus can be found are not densely populated. (Sanchez, 2024) Furthermore, underreporting may be compounded by the fact that only approximately 49.9% of public and private healthcare providers report snakebite cases to SINAVE, the national epidemiological surveillance system in Mexico. In addition, in certain regions, patients often seek traditional healers or shamans rather than medical facilities, further skewing epidemiological data. The specific snake species involved in bite incidents is not documented in official reports; however, some healthcare providers maintain internal records based on photos of the snake, or some patients even bring the dead snake. According to the authors ' experiences, Crotalus basiliscus is among the species that cause the most bites in Mexico. (Neri Castro et al., 2020)

6.3.2 Venom Composition

Crotalus basiliscus's venom mainly contains SVMPs (68%), PLA2s (14%), and SVSPs (11%). (Segura et al., 2017) There are two groups into which the Crotalus venoms can be classified: type I has high SVMP activity but low toxicity, and type II has low SVMP activity and high toxicity (LD50 < 1 µg/g). (Mackessy, 2010). It was proposed that high toxicity and high SVMP activity are incompatible. The Crotalus basiliscus venom fits in neither category, as it has an LD50 of 0,7 µg/g and high SVMP activity; therefore, an intermediate category must exist. (Segura et al., 2017)

When the venom was separated by HPLC, two peptides were identified, which matched the crotoxin acid and basic chains. (Segura et al., 2017) Crotoxin-like heterodimers, specifically an isoform of the basic chain of crotoxin with a molecular mass of 14,183 kDa, have also been isolated from the venom (Chen et al., 2004). Crotoxin-like content makes up about 3% of the proteome. PLA2s are believed to be the most lethal proteins in the venom, as mice die from respiratory paralysis, indicating neurotoxic activity. (Segura et al., 2017) According to (Segura et al., 2017), the SVSPs in the venom have no coagulant or defibrinogenating activities. Additionally, 4% SVMP-inhibitor tripeptides, 2% bradykinin-potentiating peptides, 0,6% cysteine-rich secretory proteins, and 0,2% L-amino acid oxidases are found. (Segura et al., 2017)

It is also important to note that the venom composition changes with the snake's age; PLA2s, SVSPs, and Myotoxin-a/ Crotamine were the most abundant in the smaller individuals, whereas the venom had more SVMPs in larger individuals. This study concluded that six out of 14 venoms cleaved the alpha and beta subunits of fibrinogen. The venom contained two acidic PLA2s, one basic PLA2, and one sPLA2-like myotoxin. The toxicity of the venom of smaller individuals was also higher when injected into mice, probably due to the higher concentration of Crotoxin. (Borja et al., 2025)

When comparing the electrophoretic profiles of juvenile and adult venoms, juvenile venoms have two prominent bands at 14 kDa and 10 kDa, whereas adult venoms display two prominent bands between 20 and 25 kDa. There is also variation among specimens from different locations; some venoms from Michoacán and Sinaloa lack crotoxin. Both juvenile and adult venoms can degrade the alpha and beta chains of fibrinogen. The toxicity varies among the different venoms, with samples from Michoacán exhibiting the lowest toxicity. A positive correlation exists between toxicity and crotoxin concentration, with juvenile samples having the lowest LD50 (high lethality) due to high amounts of crotoxin. (Colis-Torres et al., 2022)

Basilase is a 22 kDa enzyme found in the venom with fibrinolytic activities. It hydrolyzes the alpha and beta chains of fibrin and gamma-dimers, but at a slower rate.

Additionally, it has a strong A-alpha and B-beta fibrinogenase activity; the gamma chain was not affected by basilase. (Datta et al., 1995)

6.3.3 Alpha-2 Macroglobulin Inactivating Enzymes

Three proteinases were purified from the venom of Crotalus basiliscus that can inactivate a2M and a2AP. They have a molecular weight of approximately 23,4 kDa, 23,8 kDa, and 24,1 kDa for proteinases a,b, and c. These proteinases also exhibit fibrinogenolytic activity and induce plasma extravasation. They can degrade the alpha- and beta-chains of fibrinogen. The proteinases are metalloproteinases, and EDTA, a metal chelator, inhibits their activity. (Svoboda et al., 1995). According to their molecular weight, they belong to the P-I class of SVMPs. (Olaoba et al., 2020)

6.3.4 Toxicology

The toxicity of venoms is often studied in mice, but there is frequently a discrepancy between them and humans, as clinical manifestations can differ. (Segura et al., 2017)

As mentioned, the species is not always known at the hospital when treating snake envenomation; therefore, the effects of crotalid venom on humans are limited to a small number of case reports. One of these case reports is from Switzerland, where a 57-year-old snake breeder was bitten by his rattlesnake in the lower left leg. He experienced severe thrombocytopenia and coagulopathy and therefore received fibrinogen and tranexamic acid. Blood tests have shown low plasminogen and a2AP activity. His left leg was swollen, painful, and blistering, and he had severe rhabdomyolysis. According to this report, the most critical symptoms after severe Crotalus basiliscus envenomation are: severe coagulopathy, hemorrhage, local tissue damage, muscle necrosis, and neurological symptoms. (Meyer et al., 2017)

6.4 Thrombin Generation Assay

6.4.1 Biochemistry

The TGA is a global coagulation assay that can measure thrombin formation and inhibition. Thrombin formation is one of the most critical steps in the blood coagulation cascade. In the initiation stage, prothrombin is cleaved to thrombin via factor Xa, which is produced by the TF/factor VIIa complex. During the propagation stage, thrombin is generated in high amounts, which leads to the initiation of polymerization and stabilization of fibrin and the formation of a fibrin clot. Additionally, thrombin further activates factor V, factor VIII, factor XI, and platelets. Antithrombin is one of the primary regulators as it complexes activated clotting factor, which leaks into the plasma and does not enter the clot. As thrombin leaks into the plasma, it binds to thrombomodulin on the endothelial membrane and suppresses the procoagulant activities of thrombin. (Depasse et al., 2021)

Furthermore, the specificity of thrombin for protein C is enhanced by this binding. Protein C can enter the fibrin clot, alongside its cofactor protein S, which inactivates factor Va and factor VIIIa. (Depasse et al., 2021)

In the TGA, thrombin cleaves a fluorescent or chromogenic substrate, and the signal can be continuously measured. The output signal is proportional to the amount of thrombin generated. (Depasse et al., 2021)

There are three stages in the thrombin generation: initiation, propagation, and inhibition, which resemble the three stages in the TGA: initiation, amplification, and resolution. The initial RFU is measured over time, and with the first derivative, the initial thrombin generation curve in RFU/min is calculated. A calibration curve is used to express the generated thrombin in nM over time, which is called the thrombogram. Alongside the form of the curve, six parameters were established to interpret the TGA (Depasse et al., 2021)

- tLag (in min): time from the starting point of the reaction to the first generated thrombin
- tPeak (in min): time until the maximum amount of thrombin is generated
- Start tail (in min): time until all the thrombin is inhibited and the thrombin generation has ended.
- Peak Thrombin (in nM): maximum amount of thrombin generated
- Velocity index: corresponds to the slope between the tLag and the tPeak
- Endogenous thrombin potential (ETP): the area under the curve

6.4.2 Components

TGA can be done with platelet-poor plasma, platelet-rich plasma, frozen-thawed platelet-rich plasma, or whole blood. Since a specific blood draw is unavailable, a standardized procedure or locally established sample collection method is recommended to reduce preanalytical errors. (Depasse et al., 2021)

There are no more chromogenic TGAs on the market. The Z-Gly-Gly-Arg-AMC substrate is used for fluorogenic assays, a thrombin-specific fluorogenic substrate that produces a signal at 390 nm excitation and 460 nm emission. A mixture of TF and PL is used to trigger the thrombin generation. A very low TF and PL concentration can be used to detect hypocoagulability, such as hemophilia and factor IX deficiencies. Reagents with very low PL but higher TF concentration are suitable for thrombotic events. Higher TF and PL concentrations are used to analyze the coagulation status of patients with anticoagulant therapy. (Depasse et al., 2021)

6.4.3 Clinical Use

As a global assay, TGA can assess the procoagulant and anticoagulant mechanisms. Conventional assays are either specific for a coagulation pathway (prothrombin time for the extrinsic pathway, partial thromboplastin time for the intrinsic pathway) or a specific pro- or anticoagulant factor. These may lack sensitivity for some pathologies. The main limitation of TGA is the lack of standardization, as no commercially available

standardized reagent is available. Therefore, results differ between clinical laboratories. Several studies have analyzed the use of TGA in bleeding and thrombotic disorders. (Binder et al., 2021)

The bleeding phenotype may not correlate with the factor VIII levels in inherited hemophilia; consequently, measuring the factor VIII concentration in plasma does not reflect the coagulation capacity in patients. Emicizumab is a monoclonal antibody that binds activated factor IX to factor X and functions as a factor VIII cofactor to imitate the function of activated factor VIII. Conventional factor VIII assays will not adequately reflect its efficiency. TGA can predict the bleeding tendencies of hemophilia A patients and monitor non-factor and bypass therapies. The preferred TGA parameters are peak thrombin and the ETP. This is also the case for patients with Von Willebrand disease, as a low thrombin peak was associated with a higher bleeding risk. (Andrade et al., 2023; Binder et al., 2021)

Deep venous thrombosis is a potential clinical use in thrombotic disorders, as an elevated endogenous thrombin potential was observed in this pathology. In atherothrombosis and stroke, the hypercoagulable state was detected by TGA, the preferred parameter is the velocity index. (Binder et al., 2021)

TGA is a potential tool for assessing adequate anticoagulation and the reversal of anticoagulants in emergency situations in patients under antithrombotic therapy, such as vitamin K antagonists, direct factor Xa inhibitors, and thrombin inhibitors. (Binder et al., 2021)

6.4.4 Influence of Alpha-2 Macroglobulin

a2M is a protein consisting of four subunits of 180 kDa and is mainly synthesized in the liver, but macrophages and fibroblasts can produce it as well. Two of the four subunits are associated by covalent disulfide bonds forming a dimer, whereas two subunits are non-covalently bound to create a homo-tetramer. It is a proteinase inhibitor and an acute-phase protein because inflammatory cytokines upregulate its expression. (Lagrange et al., 2022). The plasma concentration in healthy adults is around 250

mg/100 ml, and women have a higher concentration than men. The mean concentration in children from 1-3 years is about 2.5 times higher than in adults, with 443 mg/100 ml. After that, concentration gradually decreases until the age of 30. The plasma concentration in neonates is, on average, 297 mg/100 ml, which is also higher than in adults. (Ganrot & Scherstén, 1967) In higher age groups, the concentration rises again. The a2M levels are not only affected by age and sex, but several pathologies can influence their serum levels. In immunopathological states, e.g., chronic lymphatic leukemia, the a2M levels vary widely in different patients, but there is no significant difference from healthy individuals. (Tunstall et al., 1975) In patients with diabetes mellitus, the serum levels were significantly elevated compared to those of healthy volunteers. (Yoshino et al., 2019) In hemostasis, a2M acts as an anticoagulant by inhibiting thrombin and as an antifibrinolytic by inhibiting plasmin. It can also inhibit factor Xa and activated protein C. (Lagrange et al., 2022)

a2M can inhibit several proteinases, but it mainly affects serine proteinases. The protease must be in its active form. It is suggested that the inhibition starts when the protease proteolytically attacks a2M, and the a2M molecule traps the protease irreversibly by conformational change. This ”bait” region is susceptible to attacks by proteinases. (Barrett & Starkey, 1973)

When a2M inhibits thrombin, it can still cleave small substrates. This is a problem in the TGA, as the free thrombin curve is not identical to the amidolytic activity curve. (Rijkers et al., 1998). This will impact the ETP. Some manufacturers use a mathematical algorithm to account for the impact of a2M on the ETP, but this limits the application as the levels are influenced by age, sex, and several pathologies, as aforementioned. (Ignjatovic et al., 2007) If not mathematically corrected, a residual amidolytic activity remains, making endpoint determination of the ETP difficult. (Rijkers et al., 1998)

6.4.5 Inhibition of Alpha-2 Macroglobulin

In a study by Rijkers et al. (1998), plasma was incubated with the protease from the venom of Crotalus basiliscus to inhibit a2M. A chromogenic substrate was used to determine the thrombin generation. The protease was able to inhibit a2M and reduce the residual amidolytic activity of the a2M-thrombin complex, which does not influence the blood coagulation cascade. (Rijkers et al., 1998)

7 Aim of the Thesis

The goal of this thesis was to investigate the effect of PLA2 from Crotalus basiliscus venom on blood coagulation using TGA. The snake venom was purified to produce a concentrate of PLA2s using SEC and AEC. It was evaluated whether the PLA2 in the venom is PL-dependent and if the reaction is time-dependent. Additionally, known PLA2 inhibitors were examined for their ability to inhibit the purified PLA2s in Crotalus basiliscus venom.

8 Materials and Methods

8.1 Materials

Venom

The Crotalus basiliscus venom was purchased from Latoxan (Portes lès Valence, France). 500 mg of the venom was dissolved in 4 ml of TRIS buffer (20 mM TRIS, 2 mM $CaCl_2$, pH 8) and centrifuged for 10 min at 15.000 rpm to remove non-dissolved components.

Antibodies

Primary Antibody: polyclonal PLA2 antibody purchased from Thermo Fisher Scientific (Regensburg, Germany) – host: goat, species reactivity: human, immunogen: synthetic peptide sequence (NKAHKNLDTKKYCQS) corresponding to the C-terminus of PLA2G1B

Secondary antibody: polyclonal donkey anti-goat (H+L) secondary antibody conjugated with horseradish peroxidase purchased from Life Technologies (Frederick, USA)

PLA2 Inhibitors

The PLA2 inhibitors were all purchased from Sigma-Aldrich (St. Louis, USA). The following substances were used:

- VAR (CAS: 172732-68-2)
- NIF (CAS: 21829-25-4)
- NIS (CAS: 63675-72-9)
- QUI dihydrochloride (CAS: 69-05-6)
- Rutin hydrate (CAS: 207671-50-90)
- Quercetin (CAS: 117-39-5)

8.2 Enzyme purification

8.2.1 Anion Exchange Chromatography – Alpha-2 Macroglobulin Inactivating Proteases

The enzyme purification protocol for the a2M-inactivating proteases was adapted from (Svoboda et al., 1995). 1 ml of the venom solution was loaded onto a DEAE Sepharose Fast Flow column (Cytiva, Uppsala, Sweden) with a height of 2.4 cm and a width of 1.6 cm. The proteins are eluted by applying a linear NaCl gradient from 0 to 0.4 M NaCl at a 0.5 ml/min flow rate and collected in 3 ml fractions. The fractions of the second peak were lyophilized and pooled.

8.2.2 Size Exclusion Chromatography – Alpha-2 Macroglobulin Inactivating Proteases

The fractions from the AEC with the highest activity in the plasmin inhibitor assay were used. The fraction was loaded onto a Sephacryl S-100 High Resolution column (Cytiva, Uppsala, Sweden) with a height of 92 cm and a width of 1,6 cm. The fractions (3ml) were eluted at a 0.8 ml/min flow rate and detected at UV 280 nM.

8.2.3 Size Exclusion Chromatography – Phospholipase A2

1 ml of the venom solution was loaded onto a Sephacryl S-100 High Resolution column (Cytiva, Uppsala, Sweden) with a height of 92 cm and a width of 1.6 cm. The fractions (3 ml) were eluted at a 1.3 ml/min flow rate and detected at UV 280 nM. Fractions from the second peak were lyophilized.

8.2.4 Anion Exchange Chromatography – Phospholipase A2

For the analysis of PLA2, two different AECs were carried out, one using pooled fractions 27 and 28 and another using only fraction 29. The fractions were dialyzed to a TRIS buffer (20 mM TRIS, 2 mM $CaCl_2$, pH 8.2) and loaded onto a DEAE Sepharose Fast Flow column (Cytiva, Uppsala, Sweden) with a height of 2.4 cm and a width of 1.6 cm. The

proteins were eluted by applying a linear NaCl gradient from 0 to 0.3 M at a flow rate of 0.8 ml/min and detected at UV 280 nM. The fractions with the highest PLA2 concentration were pooled and lyophilized.

8.3 SDS-PAGE

The molecular weight of the proteins in the fractions was analyzed using the NuPAGE 12% Bis-Tris Gel (Life Technologies, Carlsbad, USA). 7.5 µL of the sample was added to 2.5 µL of the NuPAGE LDS Sample buffer (Life Technologies, Carlsbad, USA) and heated to 70 °C for 10 min. 10 µL of the mixture was added to the gel alongside 5 µL of the PageRuler Prestained Protein Ladder (Life Technologies, Carlsbad, USA), and the SDS-PAGE was carried out under non-reducing conditions using the NuPage MOPS SDS Running buffer (Life Technologies, Carlsbad USA) for 45 min at 200 V, according to the manufacturer's instructions. The gels were stained with the SimplyBlue Safe Stain (Life Technologies, Carlsbad, USA), a Coomassie G-250 stain.

8.4 Western Blot

For the Western Blot, the fractions from AEC 1 and AEC 2 were diluted 1:20, and a control PLA2 from honey bee venom (Thermo Fisher Scientific, Eugene, USA) were diluted 1:10. A SDS-PAGE was carried out under reducing conditions using materials mentioned in the previous chapter and the NuPAGE Samples Reducing Agent (10x) and the NuPAGE Antioxidant by Life Technologies (Carlsbad, USA). The gel was run according to the instructions of the manufacturer.

The Proteins were electroblotted onto a Nitrocellulose Blotting Membrane (Amersham Protran Premium 0,45µM NC, Buckinghamshire, UK) at 30 V for 1 hour. Afterwards, the membrane was rinsed in a TBS-T buffer (20mM Tris, pH 8, 500 mM NaCl, 0,05% Tween 20). After the transfer, the gel was stained using the SimplyBlue safe Stain (Life Technologies, Carlsbad, USA) to assess the efficiency of protein transfer and detect residual proteins remaining in the gel. Additionally, a Dot-Blot was conducted by applying 2 µL of the fractions (1:20 diluted and undiluted) directly onto the membrane.

This method was used to eliminate potential sources of error in Western blotting, including incomplete transfer and insufficient protein concentration.

The blocking solution contained 5% dry milk powder dissolved in the TBS-T buffer, and the membranes were blocked for 1 hour at room temperature.

The primary antibody was used at a 0,01 µg/ml concentration (in TBS-T buffer with 5% bovine serum albumin). The membrane was incubated with the first antibody overnight at 4°C and afterwards washed with TBS-T buffer. The membrane was incubated with the secondary antibody at a dilution of 1:2000 (Life Technologies, Frederick, USA) for 1 hour at room temperature and washed with TBS-T buffer.

The proteins were chromogenically detected using the 1-Step Ultra TMB-Blotting Solution by Thermo Fisher Scientific (Rockford, USA).

8.5 Sequence analysis

A sequence analysis of human PLAG1B and various svPLA2s was performed to determine possible sequence homology and to assess whether the primary antibody would bind to svPLA2 in the fraction. This analysis was done with UniProt (https://www.uniprot.org).

In the first step, the alignment tool on UniProt was used, to determine the sequence homologies of different PLA2-sequences. PLA2s from the Crotalus genus and the human PLA2 detected by the primary antibody were assessed (The UniProt Consortium et al., 2025):

- PLA2 from Homo Sapiens (UniProt ID: P04054)
- Basic PLA2 F15 from Crotalus durissus terrificus (UniProt ID: P0CAS5)
- PLA2 from Crotalus atrox (UniProt ID: P0CV89)
- Basic PLA2 9 from Crotalus durissus cumanensis (UniProt ID: P86805)

The visualization of the sequence alignment was done with ESPript 3.0 (https://espript.ibcp.fr/ESPript/ESPript/). (Gouet et al., 1999)

In the second step, the peptide search tool on UniProt was used to find proteins that include the immunogenic peptide (NKAHKNLDTKKYCQS) detected by the primary antibody. (The UniProt Consortium et al., 2025)

8.6 Protein Concentration Analysis

The protein concentration of the different fractions was estimated using an ONDA spectrophotometer UV-30 Scan (Giorgio Bormac, Carpi, Italy) to measure the absorbance at 280 nm.

8.7 Plasmin Inhibitor Assay

A modified Technochrom Plasmin Inhibitor assay (Technoclone, Vienna, Austria) was used to determine the activity of the a2M-inhibiting proteases. The reagent contains plasmin, which is inhibited by a2AP and a2M. (Barrett & Starkey, 1973) As aforementioned, the SVMP in the venom of Crotalus basiliscus can inhibit both a2AP and a2M. (Svoboda et al., 1995). The assay is a chromogenic assay using the plasmin substrate Pyr-Phe-Lys-pNA.

25µL of the fractions or buffer was preincubated with 25µL of a a2M solution (100 µg/ml) for 5 min at room temperature. 50 µL of the plasmin reagent was added to the mixture, and after incubating for 90s, 50µL of the substrate was added. A complex was formed between the plasmin and a2M alongside the residual plasmin, which can cleave the chromogenic substrate and generate a signal, which can be measured at 405 nm. A higher signal was recorded if the proteases inhibit more a2M because more residual plasmin was available. The fractions must be diluted adequately to generate a linear kinetic curve.

8.8 Thrombin Generation Assay

The TGA kit from Technoclone (Vienna, Austria) was used to determine thrombin generation, which included the TGA buffer (Hepes-NaCl buffer containing bovine serum albumin), TGA substrate (Z-Gly-Gly-Arg 7-amino-4-methylcoumarin), and the TGA reagents. Different TGA reagents were used, specifically the TGA RcLow (low concentration of PL micelles and rhTF) and TGA RcHigh (high concentration of PL micelles and rhTF). The PL concentration in RcHigh was 10 times higher than RcLow. The fluorescent signal was measured at a wavelength of 360 nm/ 460 nm. The Ceveron t100 analyzer (Technoclone, Vienna, Austria) performed the pipetting steps and signal measurement. The reagents were dissolved according to the manufacturer's instructions. A calibration curve was established using the TGA calibrator kit, including the Ceveron TGA calibrator containing thrombin and a TGA calibrator buffer.

8.8.1 Inhibition of Alpha-2 Macroglobulin

The lyophilized fractions from the SEC with the highest activity, as shown in the plasmin inhibitor assay, or buffer, were added to plasma at a ratio of 1 + 9 and incubated for 10 min at room temperature. The RcLow reagent from Technoclone (Vienna, Austria) was used to determine the thrombin generation. The TGA was done with FVIII-depleted plasma or plasma with regular clotting activity. FVIII-depleted plasma was used because the a2M effect on the TGA curve is substantial.

8.8.2 Time Dependence

The pooled and lyophilized fractions from AEC 1 were diluted to 1:40, while those from AEC 2 were diluted to 1:160. Both were then mixed with the RcHigh reagent in equal parts. The final dilutions of the fractions were 1:80 and 1:320, respectively. The incubation times were 1, 10, 30, 60, 90, and 120 min. As a control, TRIS buffer was added to the RcHigh reagent in equal parts. The TGA was run according to the manual using the Ceveron t-100 (Technoclone, Vienna, Austria).

Four repetitions were made for each sample, and the TGA parameters and curve shape were then analyzed. The TGA parameters (peak, tLag, peak-time, and velocity index) of the fractions were expressed as relative values, divided by the values of the control reagent.

8.8.3 Concentration Dependence

The pooled and lyophilized fractions from AEC 1 were diluted to 1:40, while those from AEC 2 are diluted to 1:160. Five different reagents were used:

- RcLow: 1x concentration of PL
- RcHigh: 10 x concentration of PL
- Spiked RcHigh: 15 x concentration of PL
- Spiked RcHigh: 20x concentration of PL
- Spiked RcHigh: 100 x concentration of PL

20 µL of the fractions or buffer was incubated with 15 µL of each reagent for 10 minutes at room temperature. The TGA was run according to the manual using the Ceveron t-100 (Technoclone, Vienna, Austria)

Four repetitions were made for each sample, and the TGA parameters and curve shape were then analyzed. The TGA parameters (peak, tLag, peak-time, and velocity index) of the fractions were expressed as relative values, divided by the values of the control reagent.

8.8.4 Inhibition of Phospholipase A2

Six substances were selected, each with known PLA2-inhibitory activity, and dissolved in distilled water in the following concentrations:

- VAR: 0,525 mM
- NIF: 960 µM
- NIS: 856 µM
- QUI: 4,43 mM
- Quercetin: 4 mM
- Rutin: 4 mM

Initially, their influence on the TGA was established. One part of the diluted substances and nine parts of FVIII-depleted plasma were incubated for 10 minutes at room temperature. The TGA was conducted using the RcLow reagent. The curves were compared to a control plasma with one part water and nine parts of FVIII-depleted plasma.

The substances that do not affect the TGA were then selected to inhibit the PLA2 in the samples. These substances were added to the fractions at a ratio of 1:2 and incubated for 10 min. The fractions from AEC 1 had a final concentration of 1:80, and from AEC 2 of 1:160. The inhibitors were diluted 1:2. 20 µL of the fraction-inhibitor mixture was added to 15 µL of RcHigh reagent and incubated for 10 min. The TGA was run according to the manual using the Ceveron t-100 (Technoclone, Vienna, Austria).

Two control samples were used: one containing only buffer with no spiked reagent or inhibitor, and another with a fraction without inhibitor and just buffer. The sample values were divided by the values of the reagent without fractions to obtain a relative value.

Four repetitions were made for each sample, and the TGA parameters and curve shape were then analyzed. The TGA parameters (peak, tLag, peak-time, and velocity index) of the fractions were expressed as relative values, divided by the values of the control reagent.

8.9 Phospholipase A2 Activity Assay

To determine the activity of PLA2, a titrimetric method (EC 3.1.1.4) was modified. As PLA2 cleaves PL by releasing lysophospholipid and fatty acid, a change in pH can be measured. 4,0 g of solid Rabbit PLs from Berti Lab (Forlimpopoli, Italy) were dissolved in 30 ml of 1 M NaCl solution and 10 ml of 100 mM $CaCl_2$ solution. This mixture was stirred at 25 °C for three hours to form an emulsion and diluted to 200 ml with deionized water. Non-dissolved components were centrifuged and pipetted off. The pH of the emulsion was adjusted to pH 8,9 with 0,01 M NaOH using a pH meter (Orion Star A221, Thermo Scientific, USA). To determine the blank value, 0,1 ml of deionized water was added to 5,0 ml of emulsion. The reaction was run for 10 min at 25°C and maintained at pH 8,9 by adding 0,01 M NaOH. The procedure was repeated with 0,1 ml of the enzyme solution (1:200 dilution). To calculate the Units/ml enzyme, the following equation was used: (Sigma-Aldrich, 1997)

$$\frac{Units}{ml}enzyme = \frac{(Molarity\ of\ NaOH) \times [NaOH] \times 1000 \times df \times 5.1}{(T) \times 0.1}$$

[NaOH] = ml NaOH used for enzyme – ml NaOH used for Blank

df = dilution factor

1000 = conversion factor from mM to µM

T = time required to maintain the pH at 8,9 (in min)

0,1 = volume of enzyme used (in ml)

5,1 = total volume of assay (in ml)

Phospholipase A2 Inhibition

The same assay was used to examine the PLA2 inhibition capacity of the PLA2 inhibitors VAR, NIF, NIS, and QUI. The fractions from AEC 1 and AEC 2 were diluted to 1:100 and mixed with the inhibitors in equal parts. The following concentrations of inhibitors were used before mixing them with the fractions:

- VAR: 0,525 mM
- NIF: 960 µM
- NIS: 856 µM
- QUI: 4,43 mM

Therefore, when combined, the fractions and inhibitors were diluted to 1:2. This mixture was then added to the PL solution, and the assay was run as aforementioned.

8.10 Statistics and Writing Process

The permutations test analyzed the impact of the PLA2 inhibitors on the fractions. The relative values of the inhibitor parameters were compared to those without the inhibitor. R was used for data analysis.

Excel was used for all data visualization and calculating mean values and standard deviation.

The language tools ChatGPT (OpenAI, 2025) and Grammarly (Grammarly Inc., 2025) were used for linguistic support. These tools were only used for phrasing improvements and language corrections. The author did all the analyses, literature reviews, and scientific arguments.

9 Results

9.1 Inhibition of Alpha-2 Macroglobulin

9.1.1 Anion-Exchange Chromatography – a2M-inactivating Proteases

The crude venom was separated using the DEAE Sepharose Fast Flow column, and the chromatographic profile, shown in Figure 3, was obtained. The a2M-inhibiting proteases were mainly found in the first peak after the start of the NaCl gradient, indicated by arrows. Only a part of the chromatogram is shown; the full one can be found in the appendix.

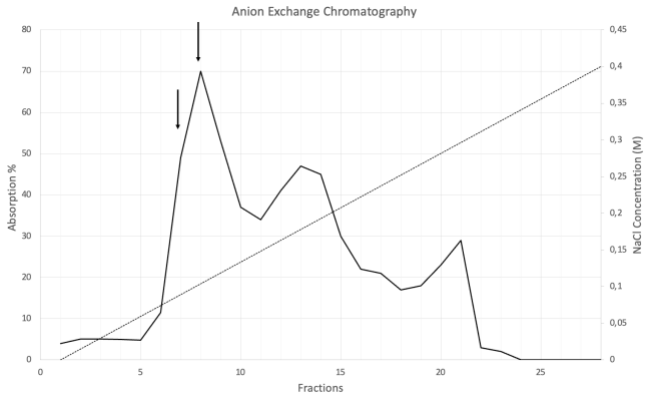

Figure 3. AEC of crude venom. Dashed line: NaCl concentration; arrows: fractions with a2M-inhibiting activity. x-axis: fractions, left y-axis: absorption in %, right y-axis: NaCl-concentration in M

9.1.2 Size Exclusion Chromatography - a2M-inactivating Proteases

The AEC fractions 7 and 8 (indicated by arrows in Figure 3) were further purified, as they had a high a2M-inactivating activity. They were pooled and applied to a Sephacryl S-100 High-Resolution column equilibrated with PBS buffer. The obtained chromatographic profile can be seen in Figure 4. The proteases were found in the first peak. A scanned copy of the chromatogram can be found in the appendix. This chromatogram has been digitized.

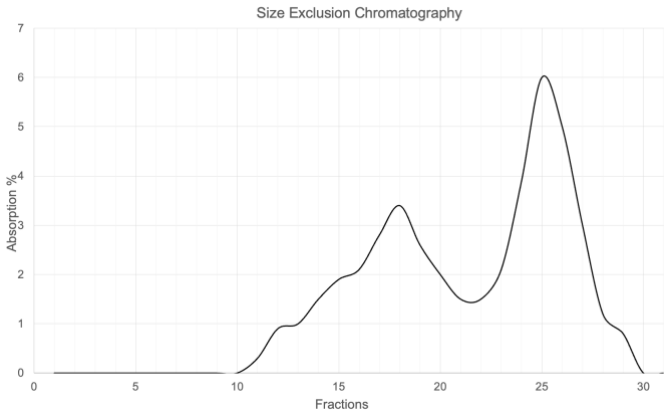

Figure 4. SEC of fraction 7 + 8 from AEC of crude venom. y-axis: absorption in %, x-axis: fractions

9.1.3 SDS-PAGE - a2M-inactivating Proteases

After the SEC step, the fractions from the first peak were analyzed using SDS-PAGE. Figure 5 shows an image of the gel. None of the fractions were pure and contained more than one protein. In fractions 17, 18, and 19, a broad band around 27 kDa and a smaller band near 10 kDa were observed. Fractions 12 through 15 contained proteins ranging from 25 to 35 kDa.

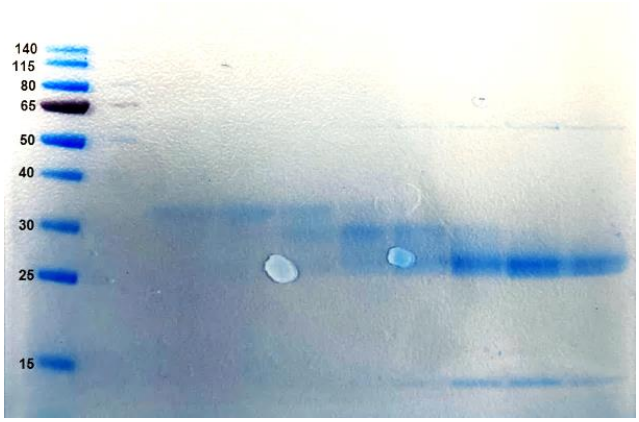

Figure 5. SDS PAGE analysis of fractions from SEC. Lane 1: molecular weight marker (in kDa); lane 3: fraction 12; lane 4: fraction 13; lane 5: fraction 14; lane 6: fraction 15; lane 7: fraction 16; lane 8: fraction 17; lane 9: fraction 18; lane 10: fraction 19

9.1.4 Protein Concentration - a2M-inactivating Proteases

The protein concentration was determined for each fraction after SEC and was as follows:

- Fraction 12: 81 µg/ml
- Fraction 13: 95 µg/ml
- Fraction 14: 113 µg/ml
- Fraction 15: 147 µg/ml
- Fraction 16: 153 µg/ml
- Fraction 17: 202 µg/ml

9.1.5 Plasmin Inhibitor Assay

After the SEC, the fractions needed to be diluted to 1:2 because their activity was too high for accurate measurement. The activity, measured in mE/min, in fractions 12, 13, 14, 15, 16, and 17 (first peak) was higher than in fraction 25 (second peak) or the buffer, as shown in Figure 6.

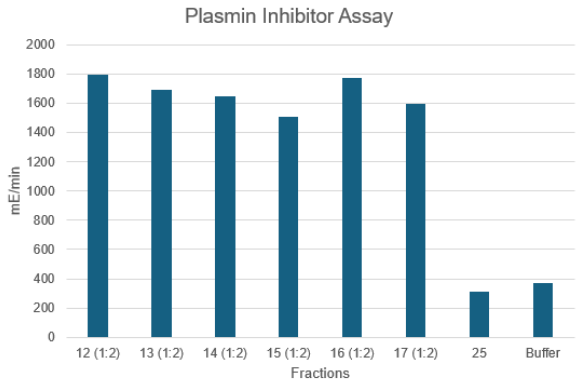

Figure 6. Plasmin inhibitor assay of fractions from SEC, diluted 1:2. x-axis: fractions, y-axis: unit (mE/min).

9.1.6 Thrombin Generation Assay - a2M-inactivating Proteases

Fractions from the SEC were incubated in FVIII-depleted plasma for 10 minutes. Fraction 17 inhibited thrombin generation, and fraction 14 slightly inhibited it (Figure 7 and Figure 9). When added to FVIII-depleted plasma, fraction 15 did not influence blood coagulation, as seen in Figure 8.

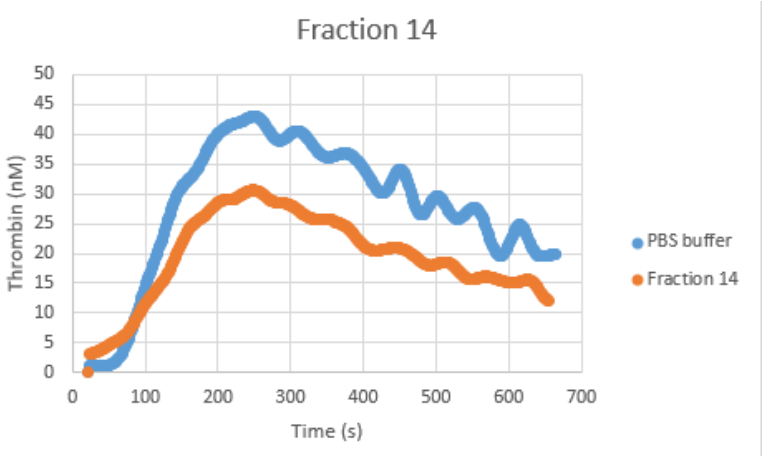

Figure 7. TGA with FVIII-depleted plasma incubated with fraction 14 for 10 min. x-axis: time in s, y-axis: thrombin in nM

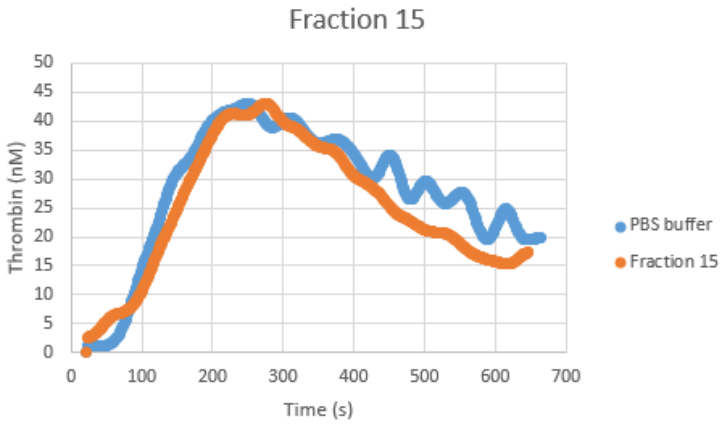

Figure 8. TGA with fraction 15 incubated with FVIII-depleted Plasma for 10 min. x-axis: time in s, y-axis: thrombin in nM

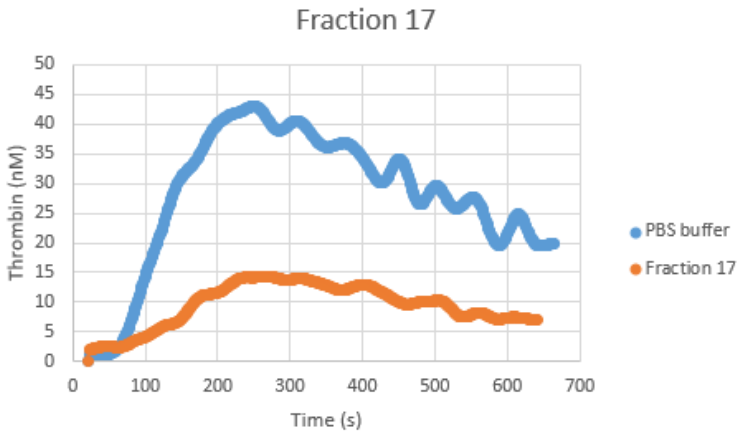

Figure 9. TGA with fraction 17 incubated with FVIII-depleted plasma for 10 min. x-axis: time in s, y-axis: thrombin in nM

Since fraction 15 did not significantly impact blood coagulation and fraction 14 only had a minor effect, the TGA was repeated using plasma with normal clotting activity. As shown in Figure 10, fraction 14 completely inhibited thrombin generation. Fraction 15 also inhibited thrombin generation, but a small signal was still observed (Figure 11).

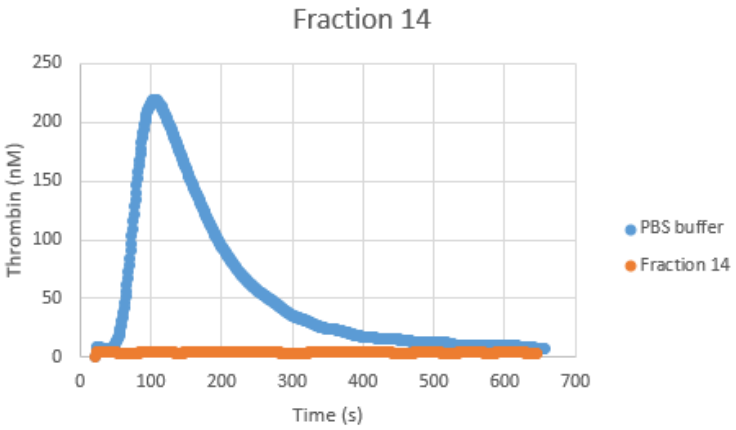

Figure 10. TGA with plasma with regular clotting activity incubated with fraction 14 for 10 min. x-axis: time in s, y-axis: thrombin in nM

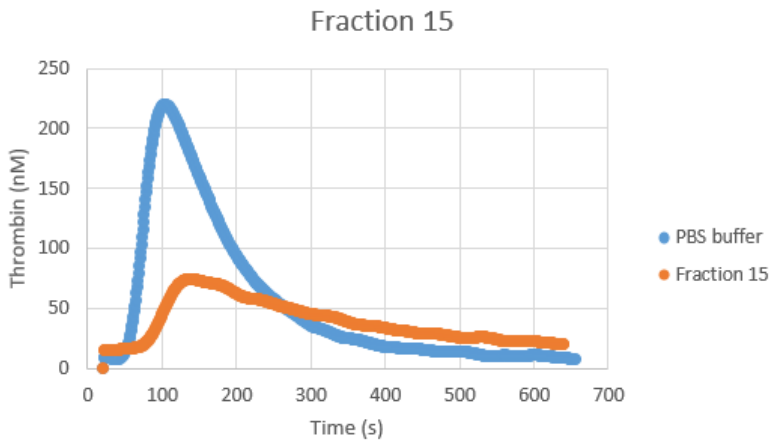

Figure 11. TGA with plasma with regular clotting time incubated with fraction 15 for 10 min. x-axis: time in s, y-axis: thrombin in nM

9.2 Phospholipase A2

9.2.1 Size Exclusion Chromatography – Phospholipase A2

The crude venom was purified using a Sephacryl S-100 High-Resolution column equilibrated with PBS buffer. The first part of the chromatogram is shown in Figure 12, with the full one in the appendix. The fractions were analyzed using SDS-PAGE, as seen in chapter 8.2.4. The fractions from the second peak were chosen for further purification, as they contained the highest amount of PLA2s. A scanned copy of the chromatogram can be found in the appendix. This chromatogram has been digitized.

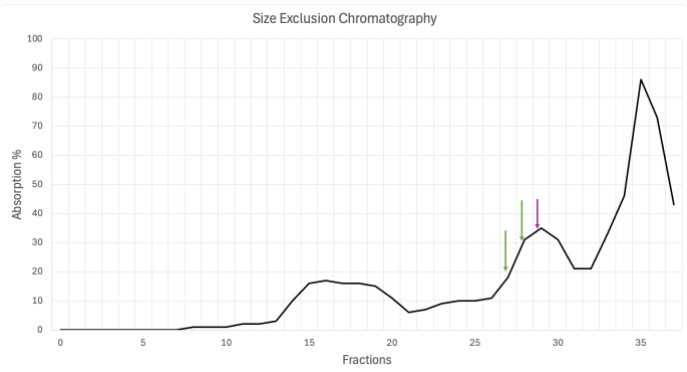

Figure 12. SEC of crude venom. In green: fractions used for AEC 1, in purple: fractions used for AEC 2. x-axis: fractions, y-axis: absorption in %

9.2.2 Anion Exchange Chromatography– Phospholipase A2

Fraction 29 and the pooled fractions 27 and 28 from the SEC were purified using a DEAE Sepharose Fast Flow column. The analyzed PLA2s are found in the second peak in both chromatograms.

Figure 13 shows the chromatogram for fractions 27 and 28, and Figure 14 shows the chromatogram for fraction 29. In both cases, fractions 28, 29, 30, and 31 were pooled, lyophilized, and contained the highest amount of PLA2s. These fractions are indicated by arrows in the figure. A scanned copy of the chromatogram can be found in the appendix. This chromatogram has been digitized.

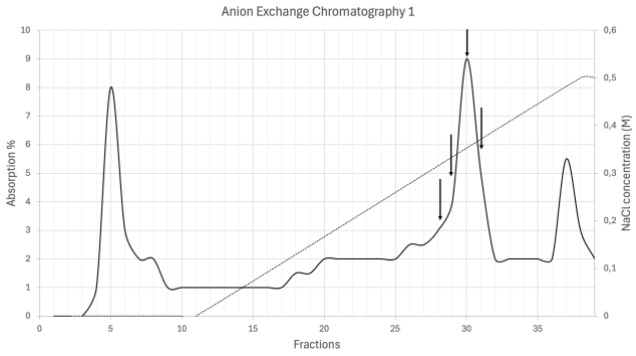

Figure 13. AEC 1 of fractions 27 + 28 from the SEC of crude venom. Arrows: pooled fractions; dashed line: NaCl concentration. x-axis: fractions, left y-axis: absorption in %, right y-axis: NaCl-concentration in M

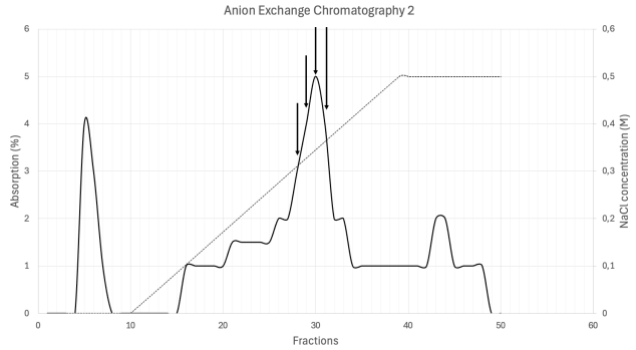

Figure 14. AEC 2 from fraction 29 of the SEC of crude venom. Arrows: pooled fractions; dashed line: NaCl concentration. x-axis: fractions, left y-axis: absorption in %, right y-axis: NaCl concentration in M

9.2.3 Protein Concentration – Phospholipase A2

The approximate protein concentration of the pooled and lyophilized fractions was as follows:

- AEC 1: 9,28 mg/ml
- AEC 2: 14,36 mg/ml

9.2.4 SDS-PAGE – Phospholipase A2

Figure 15 shows the SDS PAGE analysis of the crude venom (1:100 diluted). A broad band at around 20-25 kDa was visible, alongside bands at approximately 15 kDa, 20 kDa, 27 kDa, 30 kDa, 50 – 55 kDa, and 100 kDa.

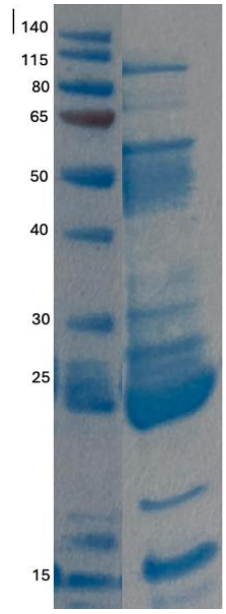

Figure 15. SDS PAGE crude venom 1:100 diluted. Lane 1: molecular weight marker, apparent molecular weight in kDa; lane 2: crude venom diluted 1:00

Figure 16 shows the SDS-PAGE analysis of the fractions after size-exclusion chromatography of the crude venom. In fractions 27 – 30, a broad band at 10-15 kDa and a band at approximately 30 kDa were visible. Fractions 27, 28, and 29 were further purified using AEC. None of the fractions were pure after the first purification step.

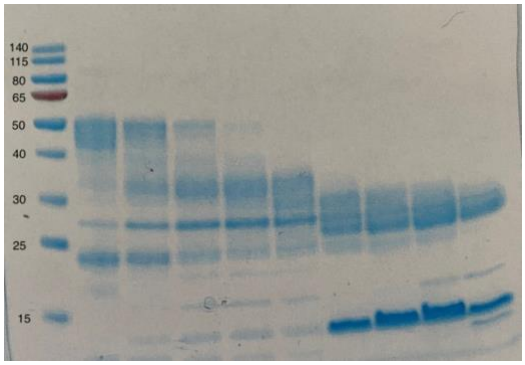

Figure 16. SDS-PAGE; Size-exclusion chromatography. First lane: molecular weight marker, apparent molecular weight in kDa, second lane: fraction 20, third lane: fraction 21, fourth lane: fraction 22, fifth lane: fraction 23, sixth lane: fraction 24, seventh lane: fraction 27, eighth lane: fraction 28, ninth lane: fraction 29, tenth lane: fraction 30

Figure 17 shows the SDS-PAGE analysis of the pooled fractions after AEC.

In the second lane, the pooled fractions from the second peak of AEC1 were applied. The most abundant proteins in the solution were 15 kDa, and a small band was seen at 30 kDa.

In the third lane, the pooled fractions from the second peak of AEC2 were applied. This lane looked similar to the second lane, with a broad band at 15 kDa and a small band at 30 kDa.

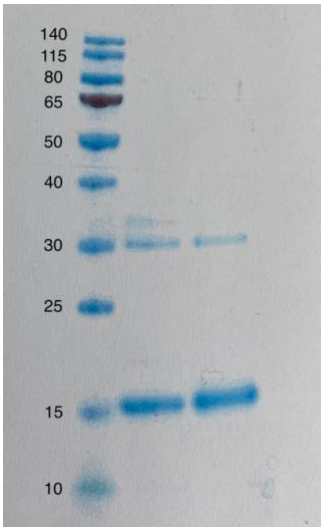

Figure 17. SDS-PAGE: pooled fractions after AEC. First lane: molecular weight marker with apparent molecular weights in kDa, second lane: AEC1, first lane: AEC 2 (1:2 diluted)

9.2.5 Western Blot and Sequence Analysis

The detection of the PLA2s in the fractions using the primary antibody specific for the human PLA2G1B and the anti-goat secondary antibody was unsuccessful. No detectable bands were observed on the membrane after the incubation with the TMB-blotting solution. The transfer of the proteins onto the gel was successful, as only minor amounts of residual proteins were detected in the gel after staining (results not shown).

In the Dot-Blot, no visible bands were observed either, indicating that transfer issues were not the cause of the error. The undiluted fractions showed no visible bands, indicating that insufficient protein concentration was not the issue. This suggested that issues with antibodies were the most probable explanation.

To assess whether insufficient binding to the PLA2 in the fractions resulted in no signal, four PLA2 sequences (three basic svPLA2 sequences from the Crotalus genus, and one human PLA2) were aligned using UniProt (https://www.uniprot.org).

It is evident that these three sequences have 50% or less homology with human PLA2, while the svPLA2s share over 75% homology (Table 1). In Table 2, the sequence alignment of the four proteins can be seen in detail.

Species	Homo Sapiens	Crotalus atrox	Crotalus durrissus cumanensis	Crotalus durissus terrificus
Homo Sapiens	100%	50,82%	37,39%	37,07%
Crotalus atrox	50,82%	100%	75,41%	78,68%
Crotalus durrissus cumanensis	37,39%	75,41%	100%	88,43%
Crotalus durissus terrificus	36,21%	78,68%	88,43%	100%

Table 1. Homology of 4 sequences using the Align-Tool on UniProt.

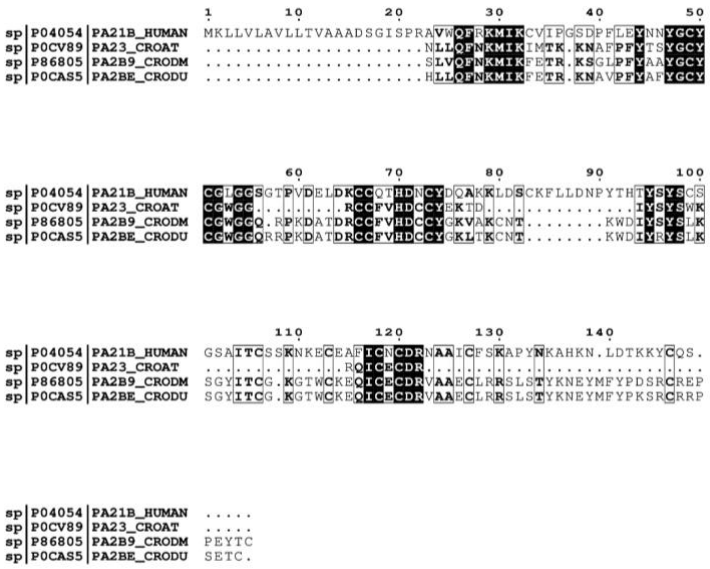

Table 2. Sequence alignment of PLA2s from the following species: homo sapiens (PA21B_HUMAN), Crotalus atrox (PA23_CROAT), Crotalus durissus cumanensis (PA2B0_CRODM), Crotalus durissus terrificus (PA2BE_CRODU). White letter with black background: amino acid identical in all sequences, bold black letter with white background: identical in at least two sequences

In the next step, a peptide search was conducted on UniProt to search for the immunogenic peptide (NKAHKNLDTKKYCQS) detected by the primary antibody.

The following proteins match the peptide sequence:

- PLA2 from Homo sapiens (UniProt ID: P04054)
- PLA2 from Pan troglodytes (Chimpanzee) (UniProt ID: A0A2J8MDS5
- PLA2 from Pan paniscus (Bonobo) (UniProt ID: A0A2R9BB84)
- PLA2 from Pan troglodytes (Chimpanzee) (UniProt ID: A0A6D2VT32)
- PLA2 from Homo sapiens (UniProt ID: F8W062)
- PLA2 from Gorilla gorilla gorilla (UniProt ID: G3QUX4)
- PLA2 from Pan troglodytes (Chimpanzee) (UniProt ID: H2Q707)

All these species are classified within the order Primates.

9.2.6 Phospholipase A2 Assay

A titrimetric assay was performed to determine the activity of PLA2 in the fractions. The AEC 1 fractions were diluted to 1:200, and AEC 2 to 1:300 to obtain a linear result. The experiment was repeated three times. The following values were obtained:

- AEC 1: 2058 U/ml
- AEC 2: 3251 U/ml

When dividing the U/ml by the protein concentration, the following values are obtained:

- AEC 1: 221 U/mg protein
- AEC 2: 226 U/mg protein

9.2.7 Thrombin Generation Assay – Phospholipase A2

Time dependence

To determine if the reaction is time-dependent, the fractions from AEC 1 were diluted to 1:40, and the fractions from AEC 2 are diluted to 1:160. They were then incubated with RcHigh reagent for 1, 10, 30, 60, 90, and 120 minutes. One curve per incubation time was selected, as shown in Figure 18 for AEC 1 and Figure 19 for AEC 2, but the experiment was repeated four times. There was a significant decrease in thrombin generation at all incubation times compared to the control. The shape of the curve differed at all incubation times compared to the control. The curve did not reach the zero point on the y-axis at its endpoint, resulting in an incomplete representation of the total area under the curve. Therefore, this parameter will not be evaluated further because it would lack methodological consistency and weaken the logical integrity of the analysis.

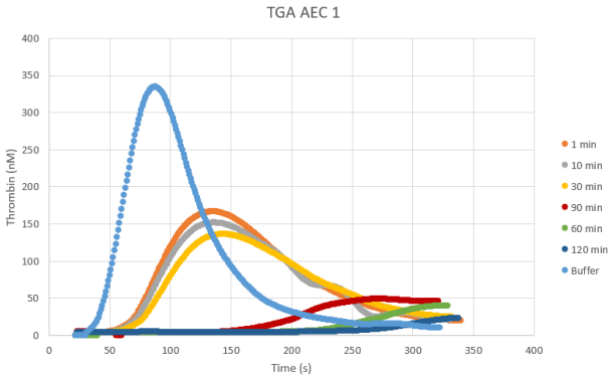

Figure 18. TGA with fractions from AEC 1 (1:40 dilution) with different incubation times: control (buffer) in light blue, 1 min in orange, 10 min in grey, 30 min in yellow, 60 min in green, 90 min in red, 120 min in dark blue. X-axis: time in s, y-axis: thrombin in nM

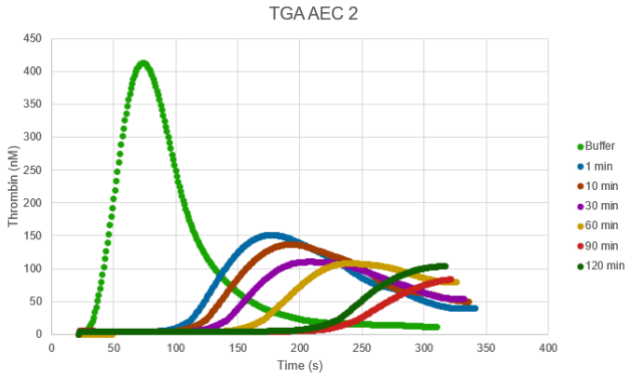

Figure 19. TGA with fractions from AEC 2 (1:160 dilution) with different incubation times: control (buffer) in light green, 1 min in blue, 10 min in brown, 30 min in violet, 60 min in yellow, 90 min in red, 120 min in dark green. X-axis: time in s, y-axis: thrombin in nM

The parameters are displayed as relative values, divided by the sample value by the value of the control curve. Figure 20 shows the mean peak values when AEC 1 was added, and Figure 21 shows the mean peak values when AEC 2 was added. Both samples decreased the peak, and the incubation time was inversely proportional to the peak value, namely, if the incubation time was increased, the peak value decreased. This correlation was stronger in the AEC 1 fractions.

The AEC 1 fractions reduced the peak value by 50% after 1 minute of preincubation, reaching an 80% reduction after 120 minutes. The decrease per minute was approximately 0.26%.

The decrease in the peak value after 1 minute of preincubation was more significant in the AEC 2 fractions, totaling about 60%, but it only reached a 70% decrease after 120 minutes. The rate of decrease per minute was slower, at approximately 0.08%.

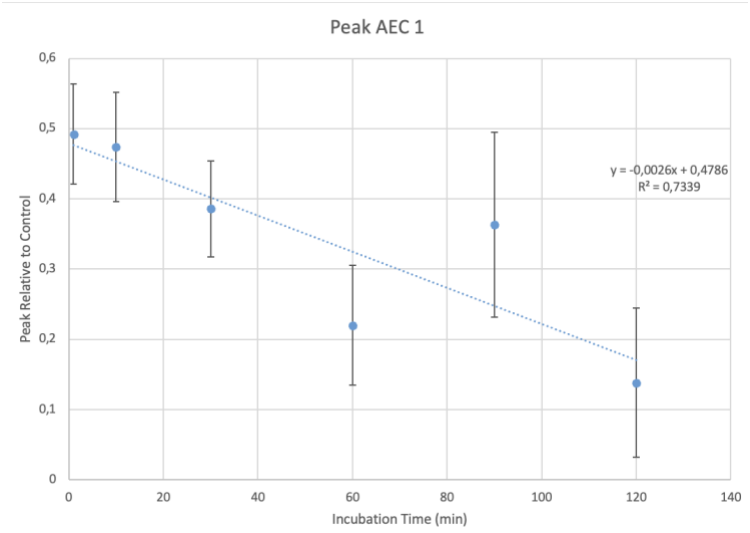

Figure 20. Peak values of pooled fractions from AEC 1 relative to the control. Plotted are the mean values and standard deviation. X-axis: incubation time in minutes, y-axis: the peak values of the fractions divided by the peak values of the control

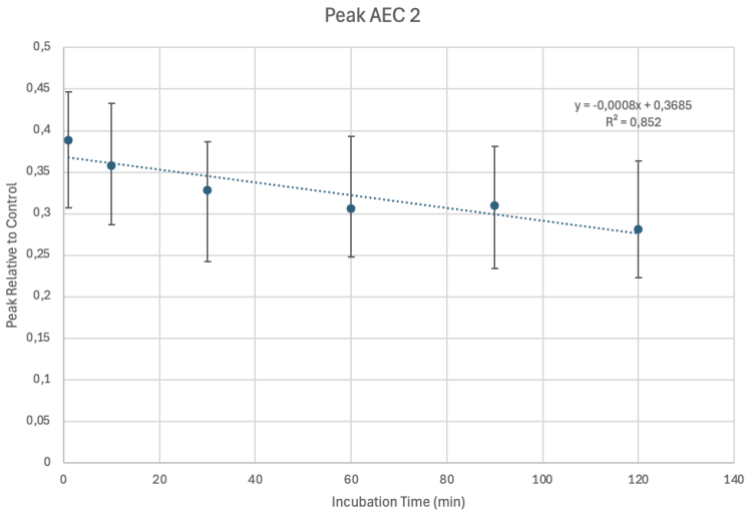

Figure 21. Peak values of pooled fractions from AEC 2 relative to the control. Plotted are the mean values and standard deviation. X-axis: incubation time in minutes, y-axis: the peak values of the fractions divided by the peak values of the control

Figure 22 shows the mean tLag values when AEC 1 was added, and Figure 23 shows the mean tLag values when AEC 2 was added, both compared to the controls. The tLag increased when the fractions were added, and the incubation time was directly proportional to the tLag values.

The tLag was twice as high as the control value after 1 minute of incubation with the fraction from AEC 1. The increase in tLag after 120 minutes exceeded 7 times compared to the controls. The AEC 2 fractions increased tLag 5 times after 1 minute of incubation and reached an 8-fold increase after 120 minutes. The trend line slope connecting the mean tLag values was similar in both figures, indicating that the rate of change is comparable, with a 3.46 % increase per minute for the AEC 1 fractions and a 2.9% increase per minute for the AEC 2 fractions.

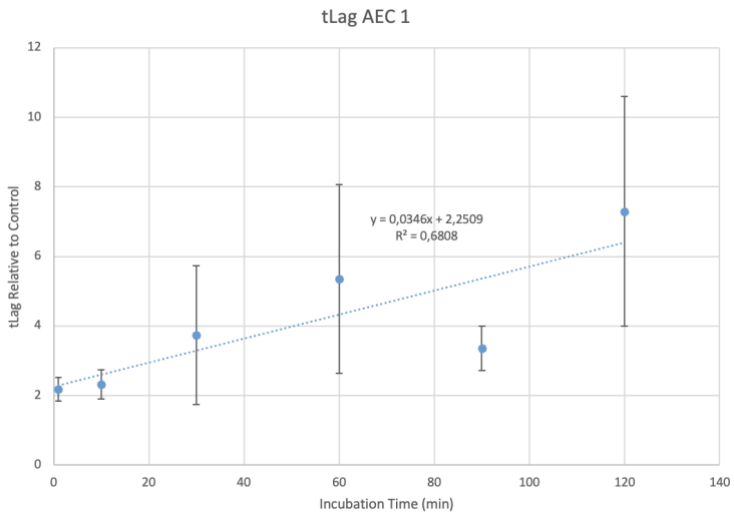

Figure 22. tLag values of pooled fractions from AEC 1 relative to the control. Plotted are the mean values and standard deviations. x-axis: incubation time in minutes, y-axis: the tLag values of the fractions divided by the tLag values of the control

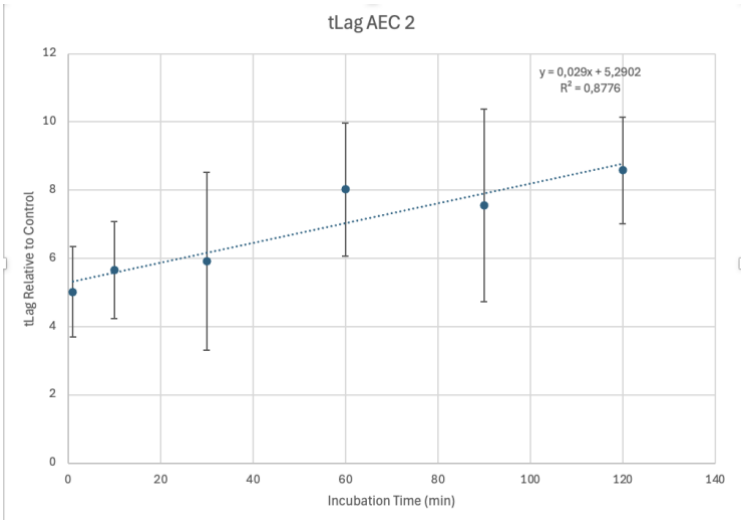

Figure 23. tLag values of pooled fractions form AEC 2 relative to the control. Plotted are the mean values and standard deviations. x-axis: incubation time in minutes, y-axis: the tLag values of the fractions divided by the tLag values of the control

Figure 24 shows the mean tPeak values when AEC 1 was added, and Figure 25 shows the mean tPeak values when AEC 2 was added. The tPeak increases as the fractions were incubated longer with the reagent. The slope of the trend line connecting the mean tLag values was similar in both figures, indicating that the rate of change was similar.

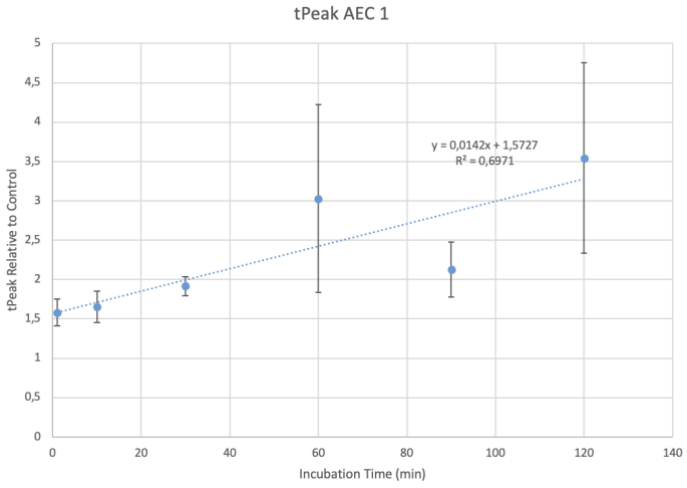

Figure 24. tPeak values of pooled fractions from AEC 1 relative to the controls. Plotted are the mean values and standard deviations. x-axis: incubation time in minutes, y-axis: the tPeak values of the fractions divided by the tPeak values of the control

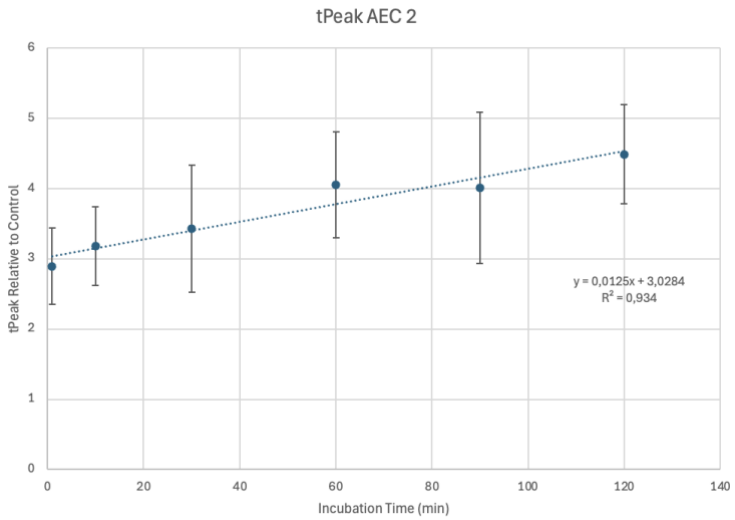

Figure 25. tPeak values of pooled fractions from AEC 2 relative to the controls. Plotted are the mean values and standard deviations. x-axis: incubation time in minutes, y-axis: the tPeak values of the fractions divided by the tPeak values of the control

Figure 26 shows the mean velocity index values when AEC 1 was added, and Figure 27 shows the mean velocity index values when AEC 2 was added. The velocity index decreased as the fractions were incubated longer with the reagent.

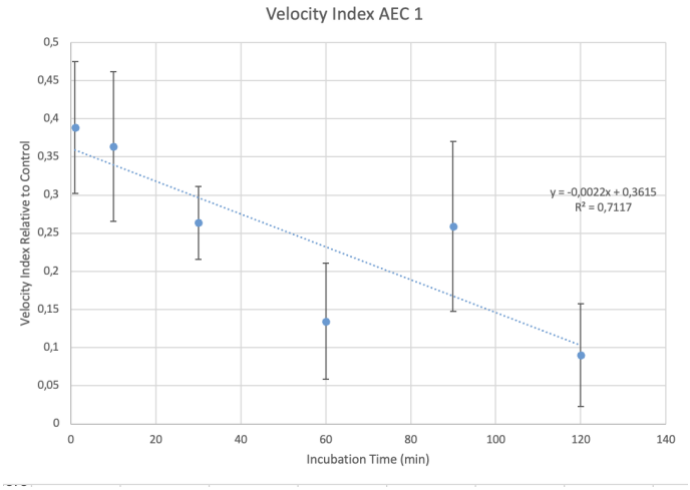

Figure 26. Velocity index values of pooled fractions from AEC 1 relative to the controls. Plotted are the mean values and standard deviations. x-axis: incubation time in minutes, y-axis: the velocity index values of the fractions divided by the velocity index values of the control

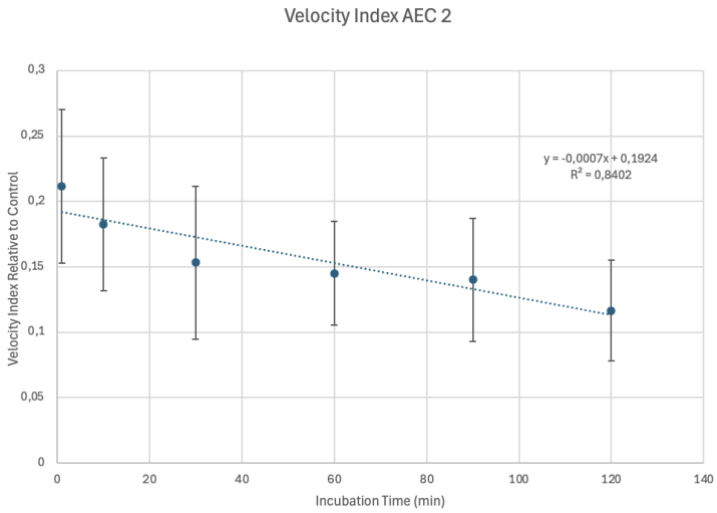

Figure 27. Velocity index values of pooled fractions from AEC 2 relative to the controls. Plotted are the mean values and standard deviations. x-axis: incubation time in minutes, y-axis: the velocity index values of the fractions divided by the velocity index values of the control

Phospholipid dependence

To determine whether the impact of the fractions on the TGA depends on the concentration of PL, the pooled fractions from AEC 1 and AEC 2 were incubated with reagents containing different concentrations of PL. The incubation time of 10 minutes remained consistent.

The RcLow reagent had the lowest concentration of PL and is labelled as 1x PL. Figure 28 shows the fractions from AEC 1 incubated with the reagent containing 1x PL, and Figure 29 shows the fractions from AEC 2 incubated with the reagent containing 1x PL. In Figure 28, thrombin generation was completely inhibited by the fractions from AEC 1, while it is only decreased when fractions from AEC 2 were added, as shown in Figure 29.

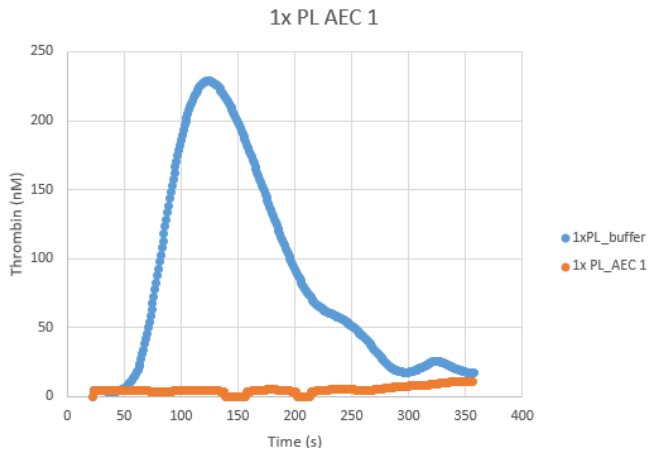

Figure 28. TGA with fractions from AEC 1 and RcLow reagent (1x PL). In blue: control (buffer), in orange: fractions from AEC 1. x-axis: time in s, y-axis: thrombin in nM

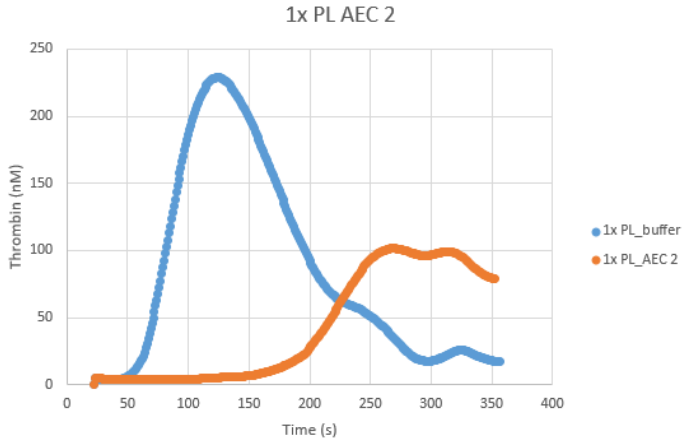

Figure 29. TGA with fractions from AEC 2 and RcLow reagent (1x PL). In blue: control (buffer), in orange: fractions from AEC 2. x-axis: time in s, y-axis: thrombin in nM

The RcHigh reagent has a PL concentration that is ten times higher than RcLow, so it is labeled as 10x PL. The thrombin generation was heavily inhibited by the fractions from AEC 1, as shown in Figure 30. The impact of fractions from AEC 2 was not as strong as from AEC 1 (Figure 31).

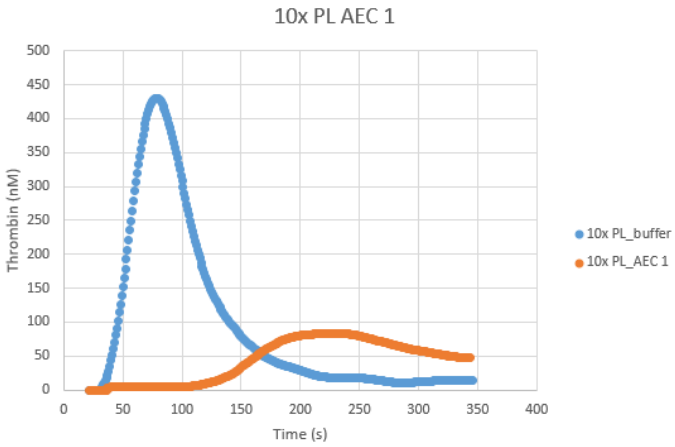

Figure 30. TGA with fractions from AEC 1 and RcHigh reagent (10x PL). In blue: control (buffer), in orange: fractions from AEC 1. x-axis: time in s, y-axis: thrombin in nM

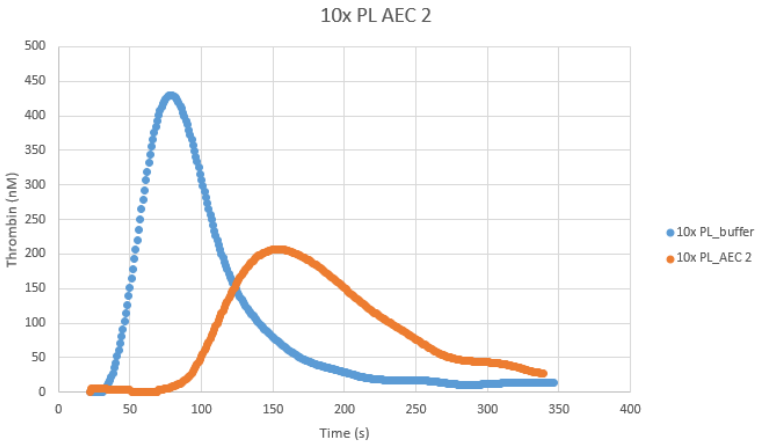

Figure 31. TGA with fractions from AEC 2 and RcHigh reagent (10x PL). In blue: control (buffer), in orange: fractions from AEC 2. x-axis: time in s, y-axis: thrombin in nM

To the 15x PL RcHigh reagent, PLs were added to reach a concentration that is 15 times higher than in the RcLow reagent, while the TF concentration remained unchanged. The difference between the TGA curves when the buffer and fractions from the AEC 1 in Figure 32 was smaller than in the 10x PL reagent. The fractions still impacted the thrombin generation. In Figure 33 with fractions from AEC 2, this effect was more pronounced, and the curves were almost equal.

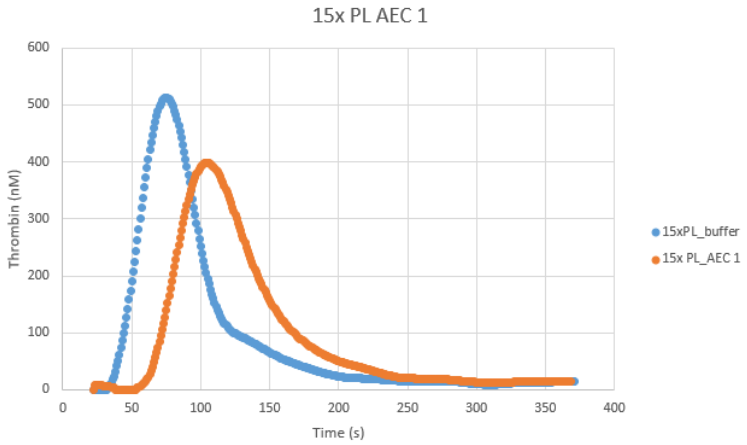

Figure 32. TGA with fractions from AEC 1 and RcHigh + PL reagent (15x PL). In blue: control (buffer), in orange: fractions from AEC 1. x-axis: time in s, y-axis: thrombin in nM

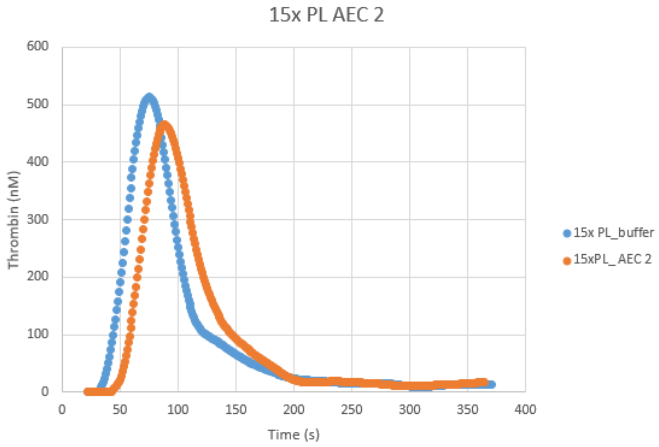

Figure 33. TGA with fractions from AEC 2 and RcHigh + PL reagent (15x PL). In blue: control (buffer), in orange: fractions from AEC 1. x-axis: time in s, y-axis: thrombin in nM.

For the 20x PL RcHigh reagent, PLs were added to achieve a concentration 20 times higher than in the RcLow reagent, while the TF concentration remained unchanged. Figure 34the TGA curves with fractions from AEC 1, and Figure 35 displays those with fractions from AEC 2. The effect of fractions from AEC 1 on the 20x PL reagent was equivalent to the 15x PL reagent. In contrast, the fractions from AEC 2 no longer affected

thrombin generation, as the curves when only buffer was added are almost identical to when the fractions were added.

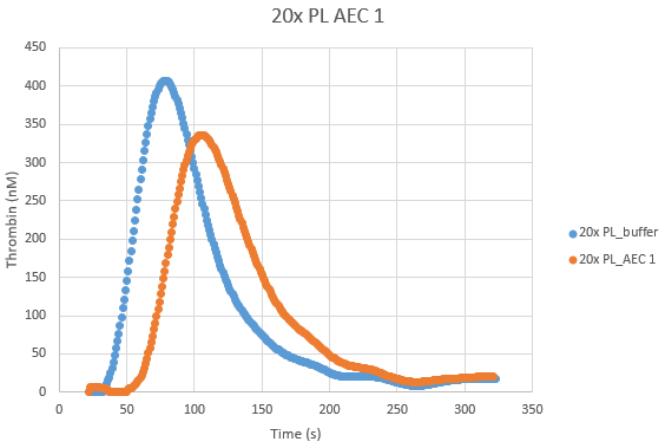

Figure 34. TGA with fractions from AEC 1 and RcHigh + PL reagent (20x PL). In blue: control (buffer), in orange: fractions from AEC 1. x-axis: time in s, y-axis: thrombin in nM

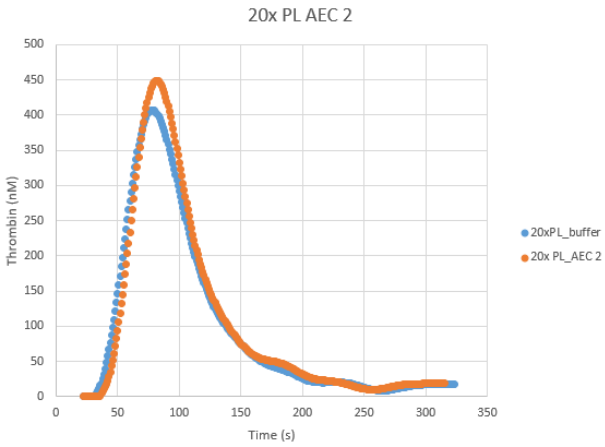

Figure 35. TGA with fractions from AEC 2 and RcHigh + PL reagent (20x PL). In blue: control (buffer), in orange: fractions from AEC 2. x-axis: time in s, y-axis: thrombin in nM

In the 100x PL RcHigh reagent, PLs were added to reach a concentration 20 times greater than in the RcLow reagent, while the TF level stayed the same. In Figure 36, fractions from AEC 1, and in Figure 37 fractions from AEC 2 were added to the 100x PL RcHigh reagent. In both figures, the curves were almost identical to the control curves.

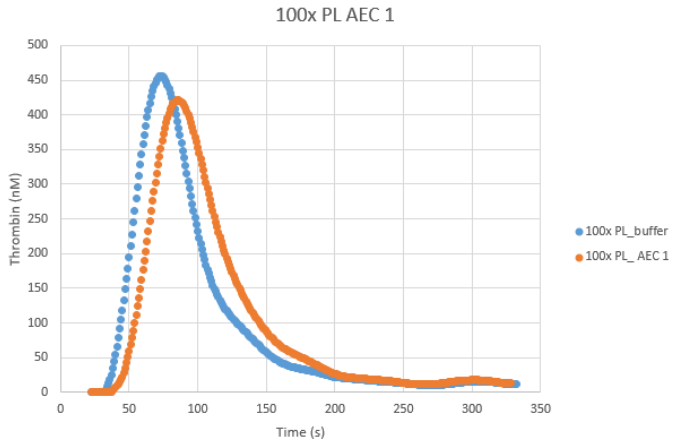

Figure 36. TGA with fractions from AEC 1 and RcHigh + PL reagent (100x PL). In blue: control (buffer), in orange: fractions from AEC 1. x-axis: time in s, y-axis: thrombin in nM

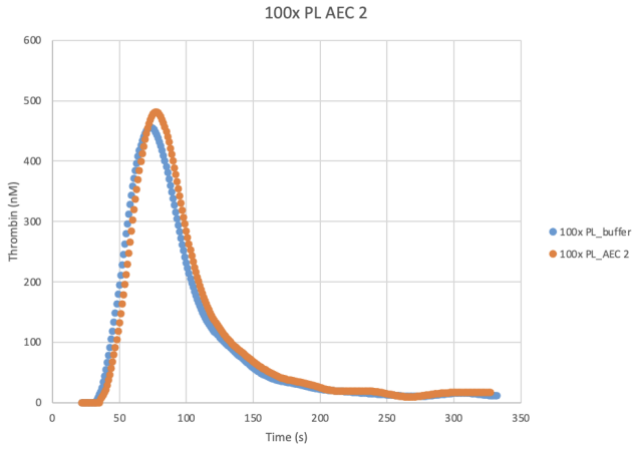

Figure 37. TGA with fractions from AEC 2 and RcHigh + PL reagent (100x PL). In blue: control (buffer), in orange: fractions from AEC 2. x-axis: time in s, y-axis: thrombin in nM

A similar trend was observed when comparing the TGA parameters. In Figure 38 to Figure 45, the values were shown relative to the control values by dividing the sample value by the control value.

When fractions from AEC 1 were added to the different reagents, the peak values were directly proportional to the PL concentrations (Figure 38). At a 15x PL concentration, the peak reached 80% of the control's peak value, and at 100x PL concentration, it exceeded 90% of the control's peak value. The peak value of the RcLow reagent (1x PL) was not assessed (shown as 0) as no thrombin generation was detected.

The peak value showed a similar pattern when fractions from AEC 2 were added to different reagents (Figure 39). A peak value was observed with the RcLow reagent (1x PL), reaching 35% of the control's peak. When the PL concentration was increased to 15 times that of RcLow, the peak surpassed 90% of the control's peak, reaching 99% with the 100x PL reagent.

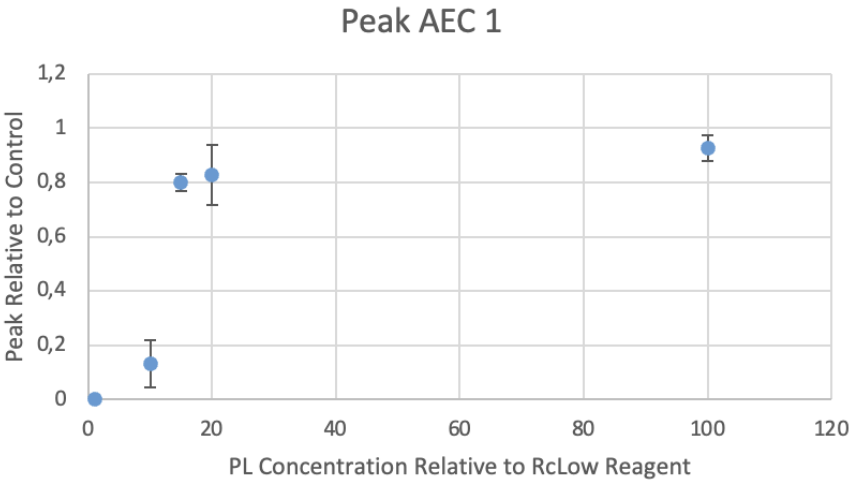

Figure 38. Peak values of pooled fractions from AEC 1 relative to the control. Plotted are the mean values and standard deviations. x-axis: PL concentration in reagent relative to RcLow reagent (1x PL-concentration), y-axis: the peak values of the fractions divided by the peak values of the control

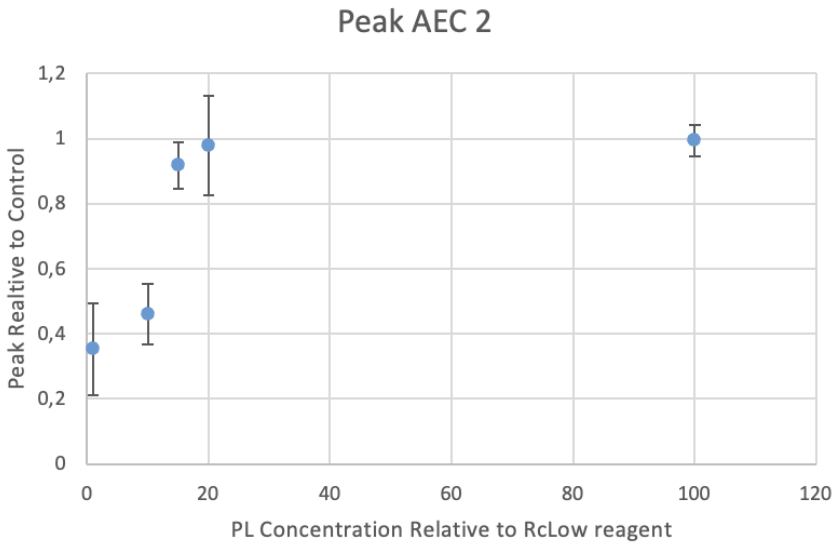

Figure 39. Peak values of pooled fractions from AEC 2 relative to the control. Plotted are the mean values and standard deviations. x-axis: PL concentration in reagent relative to RcLow reagent (1x PL-concentration), y-axis: the peak values of the fractions divided by the peak values of the control

Figure 40 shows the tLag values of the TGA when fractions from AEC 1 were added, while Figure 41 shows the tLag values of the TGA when fractions from AEC 2 were added.

The tLag value of the RcLow reagent (1x PL) was not assessed (shown as 0) as no thrombin generation was detected when fractions from AEC 1 were added. At a 10x PL-concentration, the tLag increased by over sevenfold when fractions from AEC 1 were added, while only by fourfold with fractions from AEC 2. In both cases, the tLag was nearly at the control's level at a 100x PL concentration.

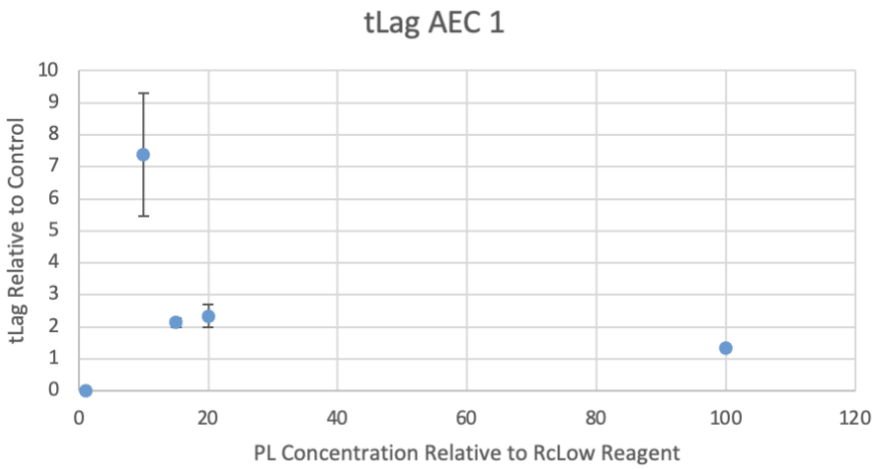

Figure 40. tLag values of pooled fractions from AEC 1 relative to the control. Plotted are the mean values and standard deviations. x-axis: PL concentration in reagent relative to RcLow reagent (1x PL-concentration), y-axis: the tLag values of the fractions divided by the tLag values of the control

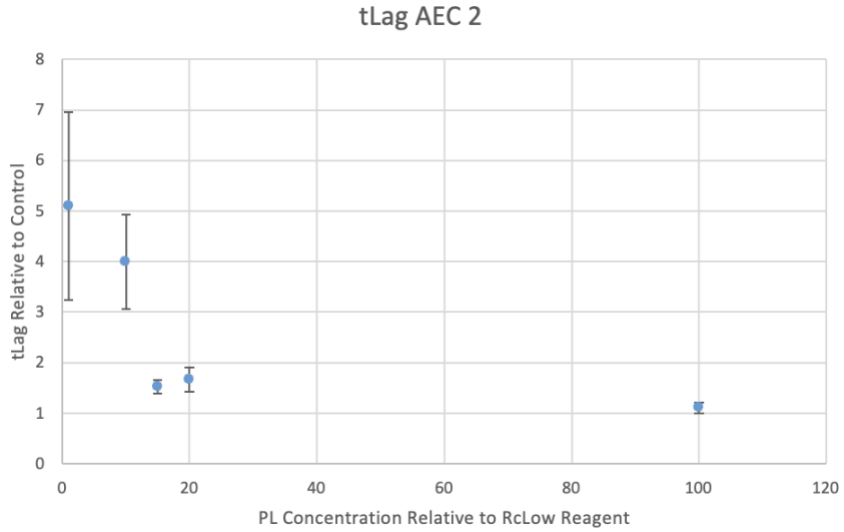

Figure 41. tLag values of pooled fractions from AEC 2 relative to the control. Plotted are the mean values and standard deviations. x-axis: PL concentration in reagent relative to RcLow reagent (1x PL-concentration), y-axis: the tLag values of the fractions divided by the tLag values of the control

Figure 42 shows the tPeak after adding fractions from AEC 1, and Figure 43 shows the tPeak after adding fractions from AEC 2; in both cases, the y-values are relative to the controls.

No tPeak was measured at 1x PL concentration because no thrombin was generated after adding fractions from AEC 1. At a PL-concentration of 100x, the tPeak nearly reached the control's value in both samples.

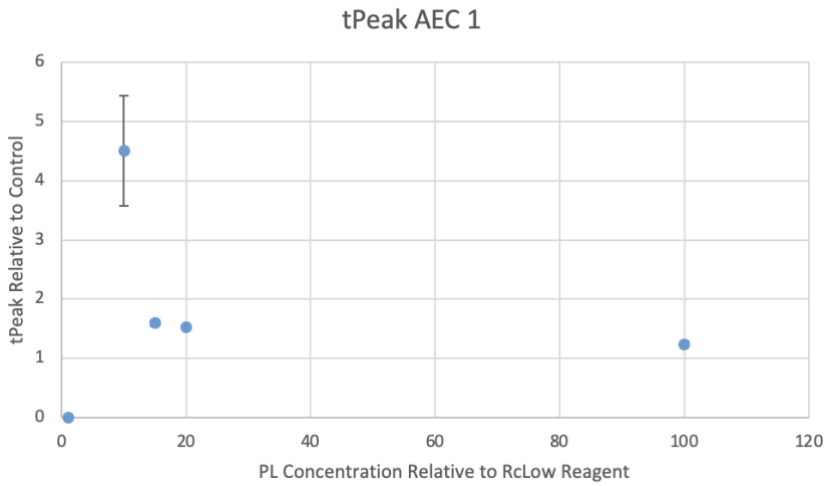

Figure 42. tPeak values of pooled fractions from AEC 1 relative to the control. Plotted are the mean values and standard deviations. x-axis: PL concentration in reagent relative to RcLow reagent (1x PL-concentration), y-axis: the tPeak values of the fractions divided by the tPeak values of the control

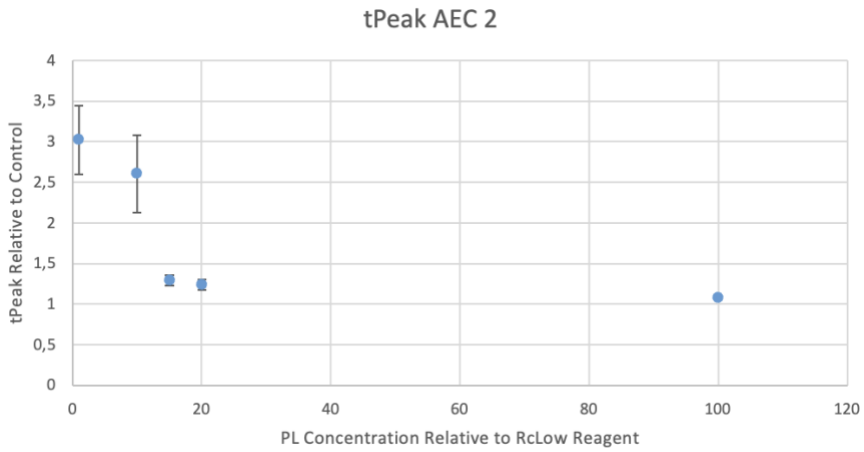

Figure 43. tPeak values of pooled fractions from AEC 2 relative to the control. Plotted are the mean values and standard deviations. x-axis: PL concentration in reagent relative to RcLow reagent (1x PL-concentration), y-axis: the tPeak values of the fractions divided by the tPeak values of the control

Figure 44 shows the velocity index values after adding fractions from AEC 1 to reagents with different PL concentrations, and Figure 45 shows the velocity index values after adding fractions from AEC 2.

The fractions from AEC 1 affected thrombin generation, and at 1x PL concentration, no velocity index value could be measured (shown as 0). At 15x PL, the velocity index exceeded 60% compared to the control value, reaching 80% when the fractions were added to 100x PL-reagents.

A similar effect was observed after adding fractions from AEC 2, with the velocity index exceeding 90% compared to the control value when fractions were added to 100x PL-reagents. When added to 15x PL-reagents, the velocity index reached 80%.

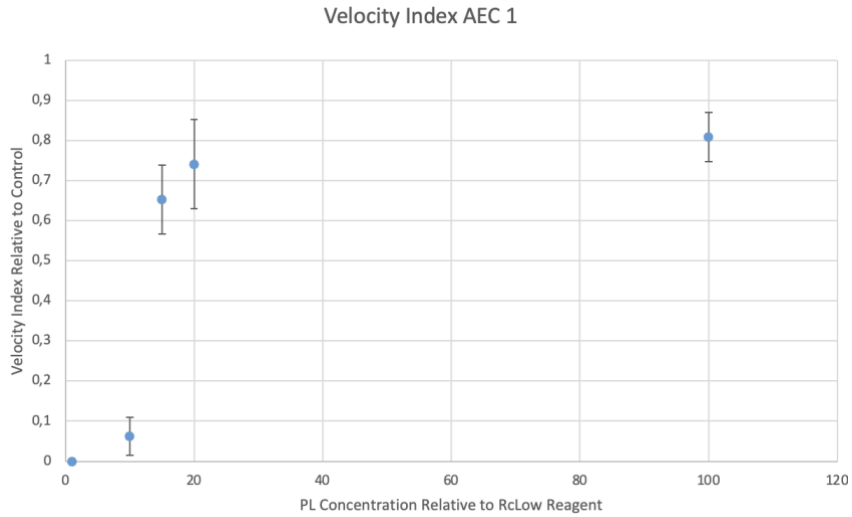

Figure 44. Velocity index values of pooled fractions from AEC 1 relative to the control. Plotted are the mean values and standard deviations. x-axis: PL concentration in reagent relative to RcLow reagent (1x PL-concentration), y-axis: the velocity index values of the fractions divided by the velocity index values of the controls

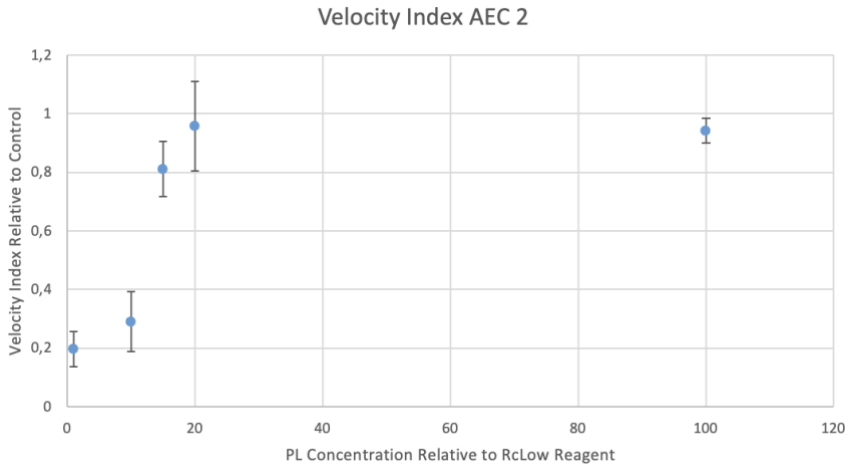

Figure 45. Velocity index values of pooled fractions from AEC 2 relative to the control. Plotted are the mean values and standard deviations. x-axis: PL concentration in reagent relative to RcLow reagent (1x PL-concentration), y-axis: the velocity index values of the fractions divided by the velocity index values of the controls

9.2.8 PLA2 inhibitors

Influence on TGA

The direct effect of various PLA2 inhibitors on TGA needed to be observed to select candidates for further testing. The inhibitors were compared to the control curve, to which water was added.

In Figure 46 NIF, and in Figure 47 NIS, were added to the RcLow reagent. Both substances had a minor effect on the TGA, decreasing the Peak and VI, while tLag and tPeak remained unaffected.

Figure 48the effect of Quercetin, and Figure 50 shows the effect of Rutin on TGA, with both substances inhibiting it.

In Figure 49, QUI was added to the RcLow reagent. It decreased the peak while increasing tLag, tPeak, and the velocity index.

Figure 51 shows that VAR did not affect the TGA.

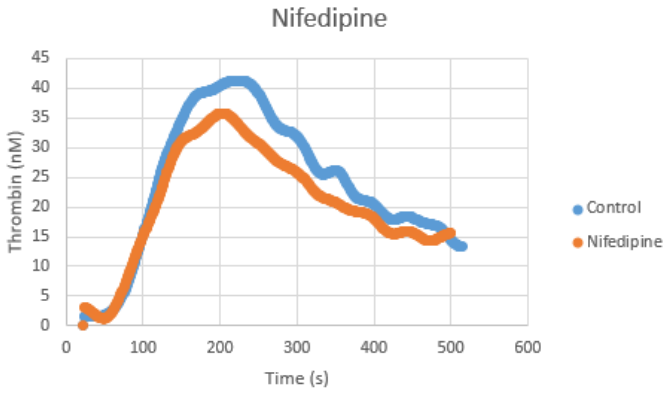

Figure 46. TGA with PLA2 inhibitor NIF (orange) and control (blue). x-axis: time in s, y-axis: thrombin in nM

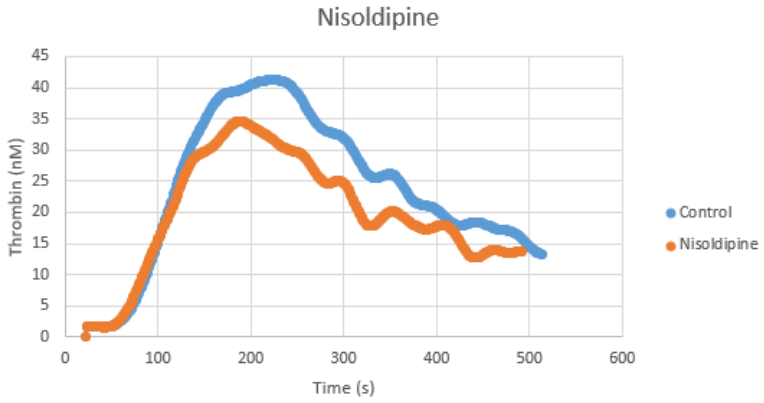

Figure 47. TGA with PLA2 inhibitor NIS (orange) and control (blue). x-axis: time in s, y-axis: thrombin in nM

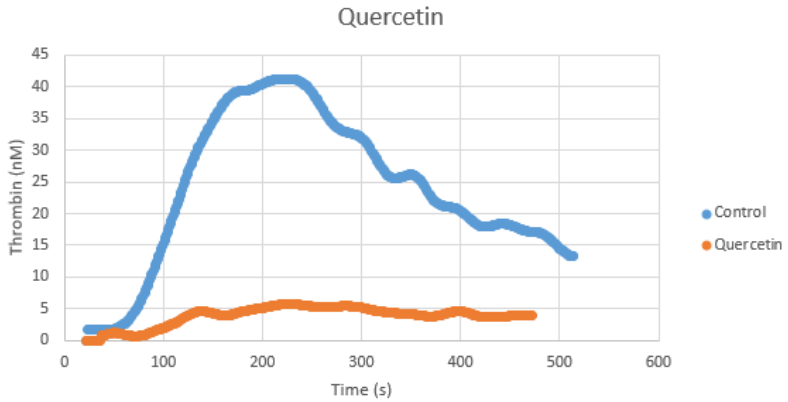

Figure 48. TGA with PLA2 inhibitor Quercetin (orange) and control (blue). x-axis: time in s, y-axis: thrombin in nM

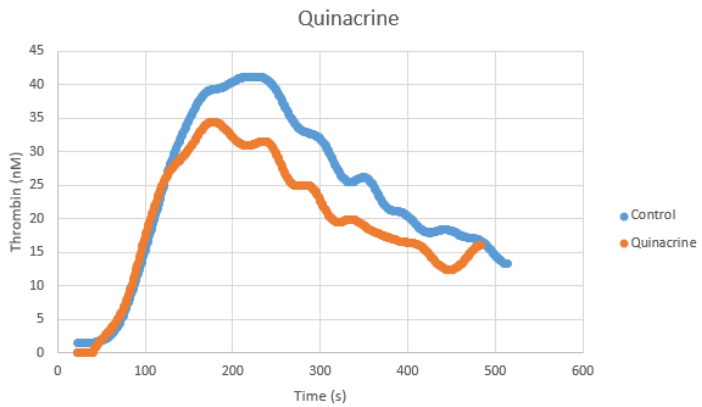

Figure 49. TGA with PLA2 inhibitor QUI (orange) and control (blue). x-axis: time in s, y-axis: thrombin in nM

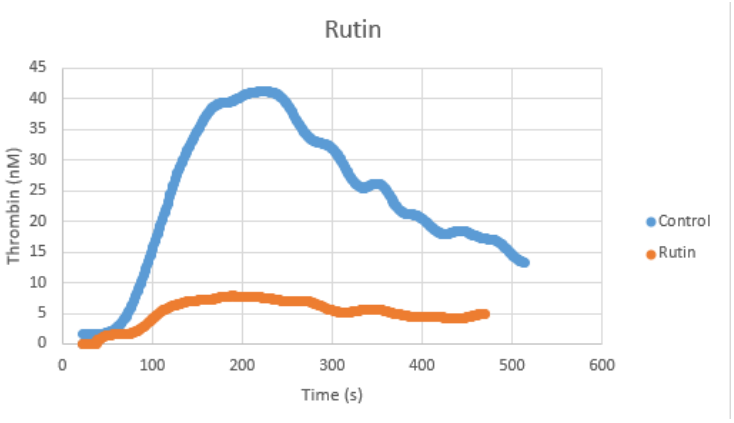

Figure 50. TGA with PLA2 inhibitor Rutin (orange) and control (blue). x-axis: time in s, y-axis: thrombin in nM

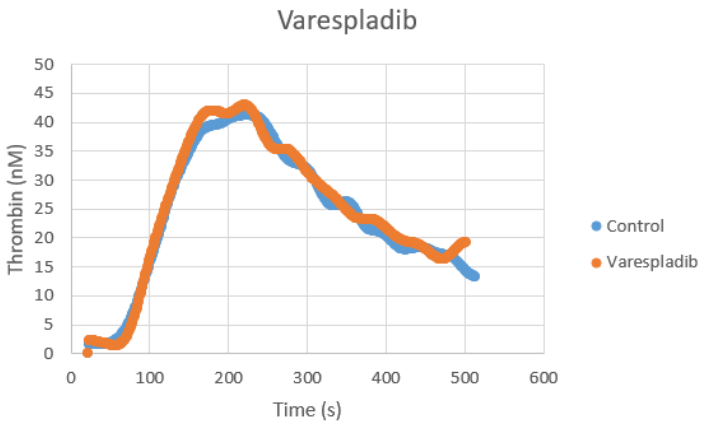

Figure 51. TGA with PLA2 inhibitor VAR (orange) and control (blue). x-axis: time in s, y-axis: thrombin in nM

Phospholipase A2 Assay

The inhibitors VAR, NIS, NIF, and QUI were chosen for further testing. The PLA2 assay evaluated their capacity to inhibit PLA2. The inhibitors were incubated with the fractions from AEC 1 or AEC 2 for 10 minutes, and their residual activity was measured using the PLA2 assay.

VAR nearly completely inhibited the PL-hydrolyzing capacity of the fractions from AEC 1 and AEC 2. NIS and QUI inhibited PLA2 in the fractions from AEC 1 by over 50%, whereas NIF inhibited them by about 28%. The PLA2s in the fractions from AEC 2 were inhibited by NIS, and NIF by over 60%, and QUI by more than 50%. (Figure 52 and Figure 53)

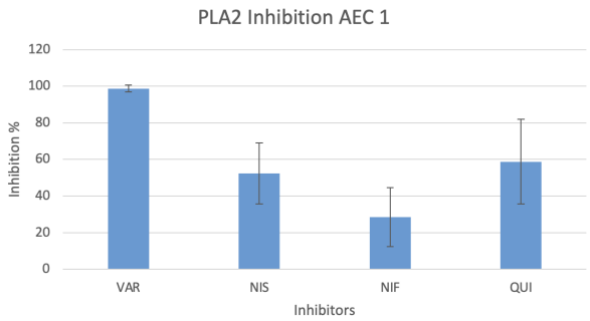

Figure 52. Inhibition of fractions from AEC 1 by PLA2 inhibitors (VAR, NIS, NIF, QUI). x-axis: inhibitors, y-axis: inhibition in %

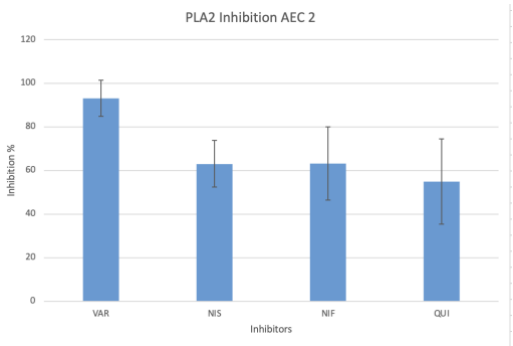

Figure 53. Inhibition of fractions from AEC 2 by PLA2 inhibitors (VAR, NIS, NIF, QUI). x-axis: inhibitors, y-axis: Inhibition in %

Inhibition of the anticoagulant effect of Phospholipase A2

Four substances, NIF, NIS, VAR, and QUI, were selected to inhibit PLA2 in the fractions from AEC 1 and AEC 2. The graphs in Figure 54 and Figure 55 are just one example of the effect of PLA2 inhibitors, the experiment was repeated four times.

The inhibitors VAR, NIF, NIS, and QUI were added to the fractions and incubated for 10 min. Two controls were used: one reagent without fractions and just buffer, and one with only fractions but no inhibitor.

Figure 54 shows the effect of different inhibitors on the fractions from AEC 1. VAR most effectively inhibited the PLA2 effect, while QUI and NIS did not influence the PLA2 inhibitory activity in blood coagulation. The impact of NIF was less significant. The curves were compared to those where AEC 1 fractions were added but no inhibitor was used (blue curve).

Figure 55 shows the effect of PLA2 inhibitors on the fractions from AEC 2. Similar to the curve in Figure 54, VAR had the most significant impact on PLA2 activity. QUI decreased thrombin generation, therefore, the PLA2 effect was not inhibited. NIF and NIS both inhibited the PLA2-induced anticoagulant activity, but the effect of NIS was more pronounced.

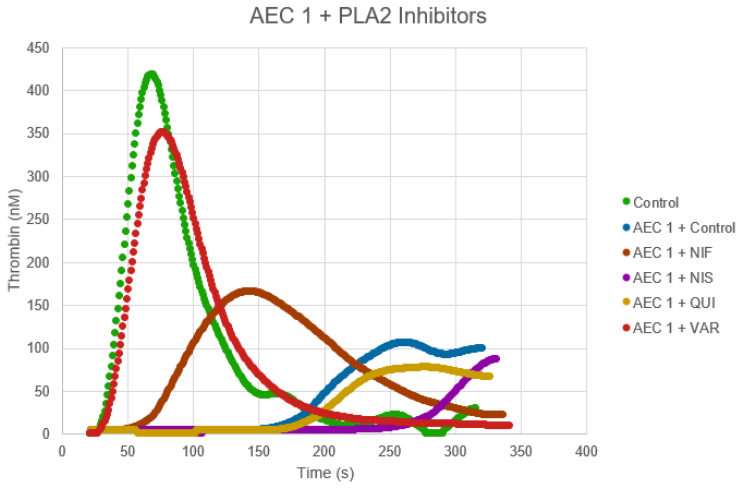

Figure 54. TGA with fractions from AEC 1 and different inhibitors: NIF (brown), NIS (violet), QUI (yellow), VAR (red), control with fractions (blue), control without fractions (green). x-axis: time in s, y-axis: thrombin in nM

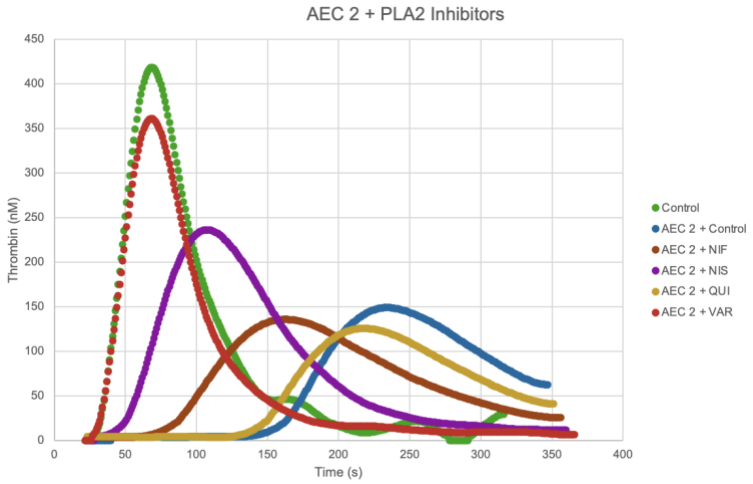

Figure 55. TGA with fractions from AEC 2 and different inhibitors: NIF (brown), NIS (violet), QUI (yellow), VAR (red), control with fractions (blue), control without fractions (green). x-axis: time in s, y-axis: thrombin in nM

In Figure 56, the peak values are relative to a control sample without added fraction from AEC 1. The control value shown in the graph represents the reagent with added fractions but no inhibitor. VAR significantly inhibited PLA2 activity ($p < 0,05$), and the peak value was almost the same as the control reagent without added fractions. QUI and NIS did not affect the inhibitory activity of PLA2 on the TGA. NIS increased the peak value to approximately 50% of the control value, but there was no significant impact on the PLA2 activity.

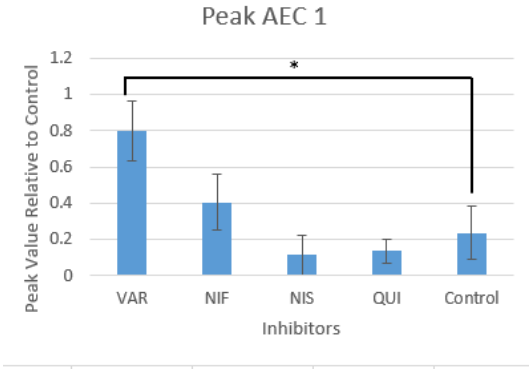

Figure 56. Peak values relative to control with fractions from AEC 1 after adding PLA2 inhibitors. The mean values and standard deviations are shown. A permutation test was performed. n=4. *, p<0.05

Figure 57 shows the effect of inhibitors VAR, NIF, NIS, and QUI on the fractions from AEC 2. When these fractions were combined with the RcHigh reagent, the peak value was decreased to about 40% of the control value with only buffer. QUI did not inhibit PLA2 activity, while NIS and NIF slightly increased the peak value, but there was no significant difference between the peaks of NIF, NIS, and the control. VAR showed the strongest inhibitory effect on PLA2, bringing the value back to that of the control reagent without added fractions.

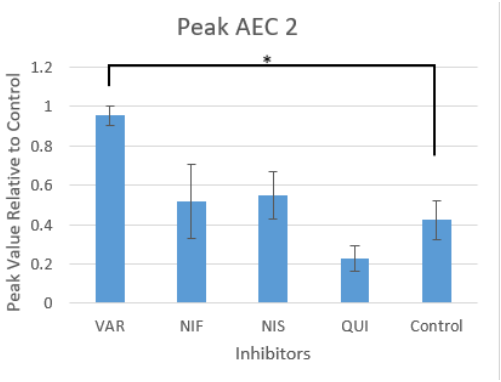

Figure 57. Peak values relative to control with fractions from AEC 2 after adding PLA2 inhibitors. The mean values and standard deviations are shown. A permutation test was performed. n=4. *, p<0.05

In Figure 58, the tLag values relative to the control samples without added fractions from AEC 1 are shown. The fractions from AEC 1 increased the tLag value by more than ten times. QUI and NIS further increased the tLag value. NIF slightly decreased it to about seven times. VAR inhibited the PLA2 activity the most, and the tLag is the same as the control reagent without added fractions. Only VAR significantly impacted the PLA2 effect on the TGA (p<0,05).

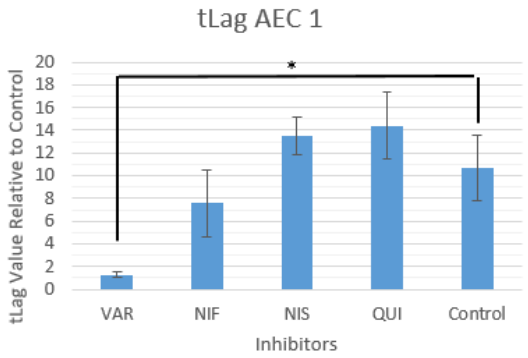

Figure 58. tLag values relative to control with fractions from AEC 1 after adding PLA2 inhibitors. The mean values and standard deviations are shown. A permutation test was performed. N=4. *, p<0.05

The tLag values after inhibiting PLA2 in fractions from AEC 2 are shown in Figure 59. The fractions increased the tLag sevenfold, and QUI raised it even more, to about elevenfold. NIS and NIF inhibited the PLA2 activity slightly, decreasing the tLag values to 3,5 times and 4,2 times, respectively. VAR inhibited the PLA2 in fractions from AEC 2 almost completely, and the tLag was equal to the tLag values of the control without added fractions. NIS and VAR significantly inhibited the PLA2 in the fractions, while QUI and NIF did not affect the PLA2 (p<0,05).

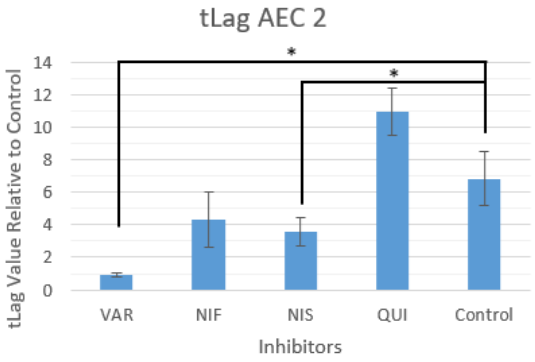

Figure 59. tLag values relative to control with fractions from AEC 2 after adding PLA2 inhibitors. The mean values and standard deviations are shown. A permutation test was performed. n=4. *, p<0.05

Figure 60 shows the tPeak values relative to the control samples without added fractions from AEC 1. The fractions from AEC 1 increased the tPeak value by over four times, as the control bar indicates. QUI and NIS further increased the tPeak value. VAR significantly decreased the tPeak value and was equal to the tPeak values of the control without added fractions (p<0,05).

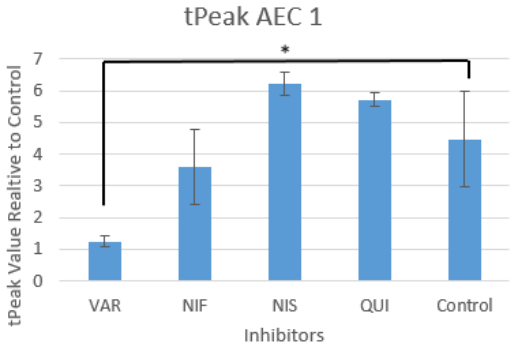

Figure 60. tPeak values relative to control with fractions from AEC 1 after adding inhibitors. The mean values and standard deviations are shown. A permutation test was performed. n=4. *, p<0.05

Figure 61shows the tPeak values relative to the control samples without added fractions from AEC 2 and the PLA2 inhibitors. NIS and VAR significantly decreased the tPeak compared to the control, with VAR having a stronger inhibitory effect. NIF and QUI had no significant impact on the PLA2 activity.

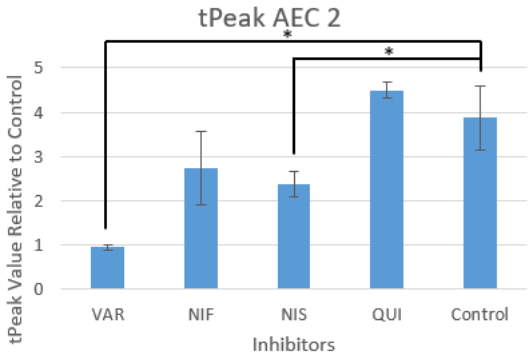

Figure 61. tPeak values relative to control with fractions from AEC 2 after adding PLA2 inhibitors. The mean values and standard deviations are shown. A permutation test was performed. n=4. *, p<0.05

The velocity index after adding fractions from AEC 1 is shown in Figure 62. VAR significantly inhibited PLA2 in the fractions, increasing the velocity index from around 10% to 70% compared to a reagent without added PLA2. NIS did not affect the velocity index, while QUI and NIF slightly increased it. This effect was not significant.

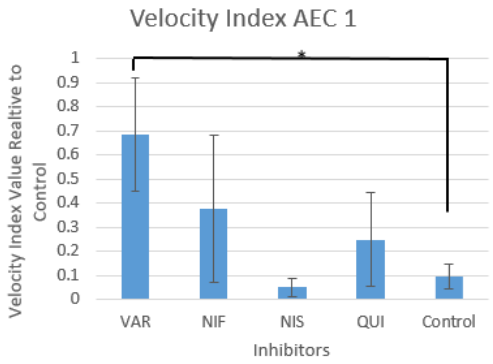

Figure 62. Velocity index values relative to control with fractions from AEC 1 after adding PLA2 inhibitors. The mean values and standard deviations are shown. A permutation test was performed. n=4. *, p<0.05

In Figure 63 the velocity index values of fractions from AEC 2 after adding PLA2 inhibitors are relative to the control value without the fractions. Only VAR significantly increased the velocity index to match the control value. NIF, NIS, and QUI slightly raised the velocity index but it did not have a significant effect on the PLA2 influence on the velocity index.

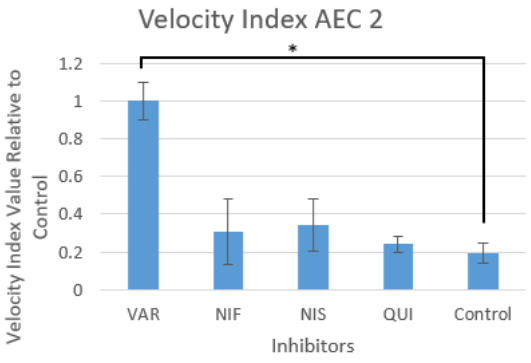

Figure 63. Velocity index values relative to control with fractions from AEC 2 after adding PLA2 inhibitors. The mean values and standard deviations are shown. A permutation test was performed. n=4. *, p<0.05

10 Discussion

In this thesis, the Crotalus basiliscus venom was further characterized using the TGA. A basic PLA2 and a2M-inhibiting proteases were chosen to investigate their influence on blood coagulation.

The a2M-inhibiting proteases were already purified by Svoboda et al. (1995), and their influence on the TGA was already established (Rijkers et al., 1998). The previous studies used a chromogenic thrombin substrate in the TGA, which is no longer standard practice. All commercial TGA kits now include a fluorogenic substrate (Depasse et al., 2021). Therefore, the influence of a2M-inhibiting proteases on the TGA with a fluorogenic substrate was investigated in this thesis.

The Crotalus basiliscus venom was characterized using a proteomic analysis by Segura et al (2017). They concluded that the venom contains 14% PLA2s, esterases that hydrolyze PL. The PLA2s in snake venoms have a molecular weight of 14-18 kDa. (Castro-Amorim et al., 2023) PLs play a crucial role in the blood coagulation cascade, in the initiation, amplification, and resolution phase of the blood coagulation (Dahlbäck, 2000; Freyssinet et al., 1986). Therefore, the anticoagulant effect of PLA2s is not surprising. The primary mechanism by which the PLA2s inhibit blood coagulation is through the hydrolysis of PL (Kini, 2005). It was also suggested that some strong anticoagulant PLA2s inhibit blood coagulation independent of PL hydrolysis by inhibiting blood coagulation factors. These reactions can be enzymatic or non-enzymatic. (Kini, 2005; Saikia & Mukherjee, 2017)

To determine whether the PLA2s in the Crotalus basiliscus venom are PL-dependent, the PL concentration in the TGA reagent was increased, and the effect was analyzed. Furthermore, the time dependency of the reaction was investigated by increasing the incubation time of the PLA2s in the TGA reagent.

Several PLA2 inhibitors have already been discovered, including VAR, NIF, NIS, and QUI. This thesis used these as controls to assess whether the anticoagulant effects are due

to the PLA2 in the mixture. Additionally, the inhibitory activity of the four substances on the PLA2s from the Crotalus basiliscus venom was evaluated.

VAR is a well-known PLA2 inhibitor that inhibits human secretory PLA2 and svPLA2. (Salvador et al., 2019) Its inhibitory effect has been confirmed for several snake venoms, including Crotalus adamanteus, Crotalus atrox, and Crotalus durissus terrificus, all of which belong to the genus Crotalus. (Lewin et al., 2016; Myers et al., 2025) However, the effect on PLA2 from Crotalus basiliscus venom has not yet been studied.

The calcium antagonists NIF and NIS inhibit the human platelet PLA2 by more than 90% (Chang et al., 1987). However, the activity against svPLA2 has never been investigated. Since svPLA2s are highly similar to human PLA2, similar interactions with small molecules are likely to occur. (Sales et al., 2017) The previous paragraph has already established this for the PLA2 inhibitor VAR.

QUI is a known PLA2 inhibitor; this effect was only demonstrated using human PLA2. It is investigated as an anti-inflammatory agent. (Çomaklı et al., 2024; Mustonen et al., 1998) Similar to NIF and NIS, this effect may also occur using svPLA2s, as QUI inhibits PLA2s by binding to them. (Mustonen et al., 1998)

The effect of the inhibitors on the TGA must first be determined to avoid interference with the anticoagulant effect of the PLA2s. Additionally, the inhibitory activity is assessed in a PLA2 activity assay based on the hydrolysis of PL and the pH measurement. The inhibitory activity in the TGA is assessed by preincubating the substances with the PLA2 and incubating this mixture with the TGA reagents.

10.1 Inhibition of Alpha-2 Macroglobulin

Crotalus basiliscus crude venom was purified using AEC (DEAE Sepharose Fast Flow column) and SEC (Sephacryl S-100 High Resolution column). The AEC produced three peaks after elution with NaCl, and the active fractions eluted early in the AEC, in agreement with previous characterizations of the a2M-inhibiting proteases. (Svoboda et al., 1995) Two fractions were further purified using SEC, resulting in two peaks. The a2M-inhibiting fractions were in the first peak.

The plasmin inhibitor assay demonstrated apparent inhibitory activity against a2M, as the measured mE/min values were higher in the fractions than when only buffer was added. Since this assay only included a2M, plasmin, and the substrate, it can be concluded that the proteins in the fractions inhibited a2M, allowing plasmin to cleave more of the substrate and resulting in a higher signal.

Figure 5 illustrates that, in fractions 17, 18, and 19, the proteases suspected to inhibit a2M were present at approximately 25 kDa, as detailed in Svoboda et al. (1995). The fractions were not pure, and a smaller band near 10 kDa was also observed. Upon comparing the electrophoretic profile of these fractions with the protein profile presented in Sánchez et al. (2020), it can be concluded that the proteins with a molecular weight of 10 kDa were likely to be PLA2s.

The initial goal of this thesis was to inhibit a2M using proteases derived from Crotalus basiliscus venom to examine its effect on TGA performance. This was previously achieved by Rijkers et al. (1998) with a chromogenic substrate. This thesis aimed to incorporate the proteases into an experimental setup using a fluorogenic substrate to obtain a similar effect while reducing the amidolytic activity to zero. For the analysis, FVIII-depleted plasma was used because its effect was more pronounced than in plasma with normal clotting activity. After a 10-minute incubation of the fractions with plasma, thrombin generation was measured. As shown in Figure 9, after adding fraction 17, thrombin generation was significantly reduced. Fraction 17 also demonstrated high a2M-inhibitory activity in the plasmin inhibitory assay. The thrombin peak was significantly reduced, and the lag phase was prolonged, indicating an anticoagulant

effect. Due to the anticoagulant activity in the fractions, the effect on the TGA performance, as shown by Rijkers et al. (1998), could not be observed. The thrombin generation was inhibited when plasma with normal clotting activity was used. This effect was believed to be due to the impurities present in the fractions, given that PLA2s are known anticoagulants.(Saikia & Mukherjee, 2017)

Since an a2M-inhibiting activity was observed in the fractions by the chromogenic assay, a potential use in TGA cannot be ruled out. The inhibition of thrombin generation should be interpreted as an effect of different venom enzymes rather than a property of the a2M-inhibiting proteases themselves. Further purification strategies should focus on the complete separation from the anticoagulant enzymes, which are most likely PLA2s. This would allow a more precise evaluation of whether a2M inactivation could serve as a correction for the residual amidolytic activity of a2M-thrombin complexes in the TGA, as proposed by Rijkers et al. (1998). This can be valuable for refining TGA measurements, especially in pathological or age-dependent variations of a2M levels. (Ignjatovic et al., 2007; Lagrange et al., 2022)

10.2 Phospholipase A2

10.2.1 Phospholipase A2 Purification and Characterization

To obtain a concentrated solution of PLA2s, the venom was purified in two steps using SEC and AEC. First, the crude venom was applied onto a Sephacryl S-100 High-resolution column. The fractions were analyzed for their PLA2 content using SDS-PAGE, with the highest amount found in the second peak.

Three fractions were selected for further purification using AEC (DEAE Sepharose Fast Flow column) with a TRIS buffer pH 8,2. The PLA2s eluted after the start of the NaCl gradient, indicating the presence of basic PLA2s. These are considered more potent anticoagulants than acidic PLA2s. (C. M. Mounier et al., 2001)

The SDS-PAGE demonstrated a clear enrichment of PLA2s after this two-step purification process. The fractions mainly contained PLA2s with a molecular weight of about 15 kDa, but impurities with a molecular weight of approximately 30 kDa were also found. Based on their molecular mass, these impurities were potentially SVSPs (Sánchez et al., 2020) or SVMPs (Olaoba et al., 2020). Although these impurities were not further characterized in this thesis, a possible impact on blood coagulation cannot be ruled out. In the future, additional purification steps, such as cation-exchange or hydrophobic interaction chromatography, can be included to remove impurities and enhance homogeneity.

The protein concentration of the pooled and lyophilized fractions of AEC 1 and AEC 2 was measured using a spectrometer by assessing the absorbance at 280 nm. The fractions from AEC 2 had a 1.5-fold higher protein concentration than those from AEC 1. Due to impurities in the solution, this value represented not only PLA2s.

No commercially available method, detection system, or reagent specifically detects svPLA2s. The Western blot analysis did not produce any detectable results using an antibody specific against human PLA2G1B. This indicated a lack of binding of the antibody, which was further supported by the in-silico sequence alignment and peptide

search. The sequence homology between human and svPLA2s from the Crotalus species is below 50%, which explains a lack of cross-reactivity. The immunogen, which is recognized by the primary antibody, is only found in mammalian PLA2s, specifically in primates, and not in svPLA2s. The absence of a detectable signal is not inconsistent with the biochemical identification but indicates antigenic variation between mammalian and viperid PLA2s.

Therefore, a direct demonstration that the enzymes in the fractions are PLA2 was impossible. The enzyme identification depended exclusively on detecting enzymatic activity and the molecular weight of the protein. Further studies need to be conducted to produce antibodies specific for svPLA2s, especially for the Crotalus genus, since the sequences are only partially similar (Table 1 and Table 2).

The PLA2 activity was characterized by its ability to cleave PL and change the pH of a solution. This assay was also an identification step, as only phospholipases can cleave PL. The fractions from both AEC had similar PLA2 activity: 221 U/mg protein and 226 U/mg protein, respectively.

10.2.2 Effect on blood coagulation

Several studies investigated the effect of PLA2 on blood coagulation. Most of them used either prothrombin time to evaluate the anticoagulant effect on the extrinsic pathway or partial thromboplastin time for the intrinsic pathway (Gutierres et al., 2022; Kini, 2005; C. Mounier et al., 1996). The TGA was never used to analyze the effect of svPLA2s on blood coagulation.

Time dependence

The time-dependent inhibition of blood coagulation was already established for PLA2s purified from different snake venoms. (Mukherjee et al., 2008) To examine whether incubation time influences thrombin generation inhibition, the fractions from AEC 1 and AEC 2 were incubated with the RcHigh reagent for 1 min, 10 min, 30 min, 60 min, 90 min, and 120 min.

Thrombin generation was significantly affected after just one minute of incubation. As incubation time increased, the peak gradually declined, and the curves generally shifted further to the left, indicating stronger inhibition. (Figure 18 and Figure 19) In Figure 18, the TGA curves with added fractions from AEC 1 are shown. No significant difference was observed among the curves for 1, 10, and 30 minutes of incubation. After 60 minutes, thrombin generation was notably inhibited by the PLA2s in the fractions from AEC 1, as only a small signal was recorded. The same effect was visible after 90 and 120 minutes of incubation, with almost no signal measured after 120 minutes. There was a significant difference between the incubation time curves at 30 and 60 minutes, indicating a time-dependent reaction. The strong inhibitory effect after a 1-minute incubation indicated an immediate reaction that develops gradually. It should be noted that the fractions were incubated with the reagent before starting the TGA. Since the assay takes approximately 45 minutes, the total incubation times always included an additional 45 minutes.

Figure 19 shows the TGA with added fractions from AEC 2. A similar effect to that of fractions from AEC 1 could be observed. The TGA was significantly affected after just 1 minute of incubation. This inhibitory effect gradually developed over time during incubation. The difference between the incubation times of 30 and 60 minutes was not as pronounced as in the fractions from AEC 1. This effect was most likely attributable to the lower concentration of the fractions from AEC 2, as they were diluted 1:160. In contrast, the fractions from AEC 1 were only diluted 1:40. The final concentrations in the reagent were 89 µg/ml for the fractions from AEC 2 and 232 µg/ml for the fractions from AEC 1.

The curves after adding fractions from both AEC 1 and AEC 2 showed a different shape compared to the control curve. This difference was more evident at longer incubation times. All curves with added fractions do not reach the zero endpoint after a run time of 3000 seconds. The part of the curve after the peak represented the resolution phase of blood coagulation. (Depasse et al., 2021) This suggested that PLA2 also affects the inhibition of blood coagulation factors. The slope in this part of the curve was less steep

than in the buffer curve. This effect became less visible at longer incubation times, as the curves became too flat.

The TGA parameters were more affected by the fractions from AEC 2 after one minute than those from AEC 1. Both samples increased the peak value, but the rate of decrease per minute was higher in the fractions from AEC 1. After 120 minutes of incubation, the peak value was greater in the fractions from AEC 2 than from AEC 1. This effect was probably due to the lower concentration of the fractions from AEC 2.

The rate of increase per minute for tLag and tPeak was similarly influenced by fractions from AEC 1 and 2. This suggests that different concentrations in the samples do not affect these two parameters. The prolongation of tLag and tPeak depended on the incubation time of the fractions. The tLag indicated the initiation stage of blood coagulation, and the tPeak indicated the amplification stage. (Depasse et al., 2021) Both stages were affected by the PLA2s in the Crotalus basiliscus venom, with tLag being more impacted. The PLA2 not only inhibited the blood coagulation but also slowed it down. These effects were all time-dependent.

Both samples reduced the velocity index, but after an incubation time of one minute, the decrease was more pronounced when fractions from AEC 2 were added. The rate of decrease per minute was higher in the fractions from AEC 1, and the velocity index reached a similar level after 120 minutes in both samples. The velocity index represented the slope of the curve between tLag and tPeak, which corresponds to the amplification phase. (Depasse et al., 2021) The decrease in this parameter indicated a significant effect of PLA2 in the venom on the amplification stage of blood coagulation in a time-dependent manner.

Phospholipid dependence

To determine whether the anticoagulant effect of PLA2 in Crotalus basiliscus venom depends on hydrolysis of PL, the PL concentration was increased to 100 times higher than in the RcLow reagent. Several PLA2 enzymes that inhibit the prothrombin complex have already been described in the literature; for example, the basic PLA2 from Naja

nigiricollis venom (Stefansson et al., 1990) and Crotoxin from Crotalus durissus terrificus (Gimenez et al., 2020). In both studies, the experimental setup included PL, which made it difficult to distinguish clearly between PL-independent and PL-dependent mechanisms. In contrast, this thesis only focused on the PL-dependency of the enzyme because the TGA, a global coagulation assay, was used, which does not allow the differentiation of the inhibition of individual coagulation factors.

Figure 28 to Figure 37 display the TGA curves with varying PL concentrations and the addition of fractions from AEC 1 and AEC 2. The fractions from AEC 1 were diluted to 1:40, and those from AEC 2 to 1:160. Both significantly influenced the lowest PL concentration, the RcLow reagent (1x PL concentration). No thrombin generation was observed when AEC 1 was added, whereas a slight signal appeared with AEC 2. A similar effect can be recorded when the fractions were added to the RcHigh reagent with a 10x PL concentration. This difference in the two fractions was likely due to the different concentrations. When the fractions from AEC 2 were added to the 20x PL reagent, there was no difference in the curve compared to when only the buffer was added. The same effect was detected at a PL concentration of 100x. This may indicate that the PL concentration was sufficiently high, the impact of the PLA2 was no longer detectable, and the enzyme had achieved its maximum hydrolysis capacity. A similar effect appeared when AEC 1 was added to the 100x PL reagent, but at 20x PL, a slight influence of the PLA2 remained detectable.

When analyzing the TGA parameters, the same result was observed. At 100x PL concentration, all parameters were close to the control level, indicating no effect of the PLA2. The TGA parameters after adding fractions from AEC 1 were significantly lower (Peak and velocity index) or higher (tLag and tPeak) when compared to the control reagent without added PLA2.

The three phases—initiation, amplification, and resolution—were all influenced by the PLA and an increase in PL concentration. The initiation stage was less affected by PLA2 when PL concentration increased, indicated by the tLag being close to the control level at 100x PL. The peak, tPeak, and velocity index trace back to the amplification stage. All

of these parameters were close to the control level at 100x PL. The influence on the resolution stage could be seen in the TGA curves. The tail reached the zero end level at 100x PL after adding PLA2. This indicated that PLA2 influences the thrombin generation and the inhibition phase of blood coagulation.

The maximum hydrolytic capacity of fractions from AEC 1 at a dilution of 1:40 lies between 20x PL and 100x PL, and for the fractions from AEC 2 at a dilution of 1:160, between 15x PL and 20x PL.

In conclusion, the findings of this thesis demonstrate that the anticoagulant effect of PLA2s in Crotalus basiliscus venom is dependent on the availability of PL. The PLA2 strongly inhibited the thrombin generation at low PL concentrations, whereas at high PL concentrations, this effect decreased. This suggests that the anticoagulant mechanism of the analyzed PLA2 was primarily mediated through the hydrolysis of PLs, rather than through alternative, PL-independent pathways. This interpretation is consistent with studies showing that basic PLA2s interact with negatively charged PL head groups. (Verheij et al., 1980)

The incomplete purity of the fractions from AEC 1 and AEC 2 may influence blood coagulation due to anticoagulant or proteolytic activity, but their specific activity was not evaluated. The clear dependence on PL concentration strongly suggests that PLA2 is the main effector.

These results confirm that TGA is a sensitive technique for analyzing PL-dependent anticoagulant mechanisms in snake venom studies.

10.2.3 Phospholipase A2 Inhibitors

Varespladib

The addition of VAR alone did not alter the thrombin generation, suggesting no influence on the blood coagulation. This was consistent with findings from the literature, demonstrating no influence on blood coagulation. (Chowdhury et al., 2024; Kazandjian et al., 2021).

At a concentration of 0,525 mM, VAR significantly altered the thrombin generation compared to the control curve with added fractions from AEC 1 and AEC 2. The peak and velocity index were significantly increased, and the tPeak and tLag significantly decreased. The findings from the TGA were consistent with those from the PLA2 assay, demonstrating a near-complete inhibition of PLA2 in the fractions. The results were in agreement with previous studies showing that VAR blocks the interaction of fatty acids with the hydrophobic channel. (Salvador et al., 2021)

Nifedipine and Nisoldipine

NIF and NIS had a minor influence on the thrombin generation when added to FVIII-depleted plasma. Despite this, the two calcium antagonists were included in the further studies.

In the PLA2-Assay, both substances exhibited PLA2-inhibitory activity. The PLA2 activity in fractions from AEC 1 was inhibited by over 20%, and in fractions from AEC 2 by over 50%. This suggests an effect on the PL-hydrolyzing activity of the PLA2 in the fractions.

NIS significantly reduced the tLag and tPeak values when fractions from AEC 2 were added, although the effect was less pronounced compared to VAR. NIF did not significantly affect the inhibitory activity of PLA2 in the TGA. The activity of fractions from AEC 1 was higher than that from AEC 2, as indicated by the differences in TGA parameter values in the control groups. This may explain the different effects of NIS on the two samples. Increasing the concentration of NIS in samples with added fractions from AEC 1 might affect the inhibitory activity; however, such experiments were not

conducted. At a concentration of 856 µM, NIS significantly decreased the values of tLag and tPeak after adding fractions from AEC 2, compared to the control curve.

Quinacrine

QUI slightly decreased thrombin generation when added to FVIII-depleted plasma. Despite this, the substance was included in further studies because the effect was minor.

In the PLA2 assay, QUI inhibited the PLA2 in the fractions from AEC 1 and AEC 2 by over 50%, suggesting a significant impact on the hydrolyzing capacity of the PLA2.

In the TGA, QUI did not affect the effect of the AEC 1 and AEC 2 fractions on thrombin generation. There was no significant difference between the TGA parameter values of the control and the samples with added QUI. This suggested that QUI was ineffective at inhibiting the PLA2 in the Crotalus basiliscus venom.

Due to limited time and resources, the inhibitors were tested at only one concentration. Further studies are needed to determine whether QUI and NIF exhibit inhibitory activity at higher concentrations in the TGA. Increasing the concentration of NIS could lead to more effective inhibition. Additionally, differences in solubility, plasma binding, or target accessibility could also contribute to an incomplete reversal of anticoagulation.

10.3 Limitations

The first limitation of this thesis was the lack of previous research studies. Some studies have identified different protein classes in the Crotalus basiliscus venom, but only a few of them were investigated in more detail. The anticoagulant activity of svPLA2 was already characterized in detail, but with conventional clotting assays such as the prothrombin time, thrombin time, and activated partial thromboplastin clotting time, not TGA.

The second limitation of this thesis was the insufficient purification of the fractions. Impurities of unidentified proteins were present in every sample, and due to a lack of time and resources, these were not investigated. The venom of Crotalus basiliscus has not been well studied, so an identification based on molecular weight was not possible either. The influence of these impurities on blood coagulation and thrombin generation is unknown. This problem could be solved using different chromatography methods, e.g., hydrophobic interaction chromatography or HPLC instead of LPLC.

Using chromatography to purify snake venoms is inherently limited, as many proteins must be separated. In the AEC, the different protein classes may interact with each other and influence the charge needed for the separation. In the SEC, adhesion to other proteins may occur, leading to a higher molecular weight and incorrect purification.

Another limitation of this thesis was the small sample size. Because of limited reagents and sample volume, most experiments were repeated only four times, which is not enough for reliable statistical analysis. A statistically significant relationship may have been overlooked, especially in the activity of PLA2 inhibitors.

Due to limited resources and time, the PLA2 inhibitors were only tested at one concentration in the TGA. The PLA2 assay indicates strong inhibitory activity for all tested substances (VAR, NIS, NIF, QUI). Further experiments need to be conducted using higher concentrations of NIS, NIF, and QUI to determine PLA2 inhibition in the TGA.

Additionally, it was not possible to directly demonstrate that the proteins in the fractions were PLA2, as no commercially available method was accessible. There are only primary antibodies specific for human PLA2s but not svPLA2s available, making detection using Western Blot or Dot Blot impossible. Further studies need to be conducted using more specific detection methods.

11 Conclusion

This thesis examined the effect of PLA2 from Crotalus basiliscus venom on blood coagulation using TGA. It was shown that the basic PLA2 in the venom inhibited thrombin generation in a PL- and time-dependent manner. The PL hydrolytic effect was confirmed through the PLA2 assay and further supported by increasing the PL concentration in the TGA reagents. The time dependency was confirmed by increasing the incubation time. All these anticoagulant effects could be detected using TGA.

The venom of Crotalus basiliscus was further characterized by confirming the existence of a2M-inhibiting proteases, first discovered by Svoboda et al. (1995), and basic anticoagulant PLA2s. This Mexican rattlesnake has not been studied thoroughly, and this thesis can give more insight into the pathological mechanisms of intoxications caused by snake bites. VAR inhibited the anticoagulant effect of the PLA2 in the Crotalus basiliscus venom. Another svPLA2 inhibitor, the calcium-antagonist NIS, was discovered in this thesis. Both substances significantly altered the inhibitory effect on thrombin generation.

SVMPs from Crotalus basiliscus venom significantly inhibited a2M in the plasmin inhibitor assay. This indicates a potential application in the TGA, as demonstrated by Rijkers et al. (1998). The high zero end level measured in the TGA, which can be attributed to the a2M-thrombin complex, may decrease if these proteases inhibit a2M. (Hemker et al., 2007) This desired effect was not observed in this study, possibly due to various reasons that could be addressed in future research. The impurities in the fractions, identified as PLA2 based on molecular weight, cause an anticoagulant effect. The purification methods need to be adjusted to obtain preparations of higher purity. It is also likely that the concentration of the proteases was too low in the preparations obtained by the purification methods used in this study, resulting in insufficient inhibition of a2M. Further studies are needed to obtain a conclusive result on whether the proteases can improve performance of the TGA.

A basic PLA2 with a molecular weight of approximately 15 kDa was purified from the Crotalus basiliscus venom. This PLA2 had anticoagulant properties, which were investigated using the TGA. Two different samples were obtained after purifying different fractions from SEC using AEC. The composition of the two samples was likely very similar, as the SDS-PAGE and the impact on the thrombin generation were virtually identical. The influence of the investigated PLA2 on the blood coagulation was PL-, and time-dependent. The TGA parameters decreased (Peak and Velocity Index) or increased (tLag and tPeak) when the incubation time of the PLA2 was increased. To determine whether the PLA2 is PL-dependent, the PL concentration was increased in the TGA reagent. The PLA2 had the greatest effect on the reagent with the lowest PL concentration, and at a 100x PL concentration, no impact on thrombin generation was observed for either sample. The maximum hydrolytic capacity of fractions from AEC 1 at a dilution of 1:40 lay between 20x PL and 100x PL, and for the fractions from AEC 2 at a dilution of 1:160, between 15x PL and 20x PL. The two samples did not have the same concentration, which affected the ability to hydrolyze PL. The influence of the PL concentration on the anticoagulant properties of the PLA2 suggested a PL-dependency. The PLA2 activity was measured using a test based on PL hydrolysis, which provided additional evidence that the anticoagulant effect of PLA2 was mediated by PL hydrolysis. The fractions contained impurities of unidentified proteins, which may influence the thrombin generation. Further studies need to be conducted to determine the exact hydrolytic capacity, and different purification methods need to be applied to remove the impurities.

VAR and NIS could inhibit the anticoagulant effect of the PLA2 in the Crotalus basiliscus venom. Both inhibitors significantly affected the impact of PLA2 on thrombin generation. VAR was more effective at inhibiting PLA2 activity than NIS at the concentration used. Further studies need to be conducted to determine whether NIF and QUI have an inhibitory activity as well and at which concentrations.

This thesis indicates a potential role for TGA in investigating the hemostatic effects of PLA2 after snake bites and the changes during the treatment. The hydrolysis of PL, the

central mechanism underlying the anticoagulant effect of PLA2, can be measured with high sensitivity with the TGA. This makes it a suitable analytical tool for characterizing the pathophysiological effects of different snake venom proteins and as a diagnostic tool in clinical practice for cases of envenomation.

12 References

Andrade, P. E. A., Manucci, P. M., & Kessler, C. M. (2023). Emicizumab: The hemophilia A game changer. *Haematologica*, 0–0. https://doi.org/10.3324/haematol.2022.282099

Barrett, A. J., & Starkey, P. M. (1973). The interaction of α2-macroglobulin with proteinases. Characteristics and specificity of the reaction, and a hypothesis concerning its molecular mechanism. *Biochemical Journal*, *133*(4), 709–724. https://doi.org/10.1042/bj1330709

Binder, N. B., Depasse, F., Mueller, J., Wissel, T., Schwers, S., Germer, M., Hermes, B., & Turecek, P. L. (2021). Clinical use of thrombin generation assays. *Journal of Thrombosis and Haemostasis*, *19*(12), 2918–2929. https://doi.org/10.1111/jth.15538

Borja, M., Castañeda-Gaytán, G., Alagón, A., Strickland, J. L., Parkinson, C. L., Gutiérrez-Martínez, A., Rodriguez-López, B., Zarzosa, V., Lomonte, B., Saviola, A. J., Fernández, J., Smith, C. F., Hansen, K. C., Pérez-Robles, A., Castañeda-Pérez, S., Hirst, S. R., Olvera-Rodríguez, F., Fernández-Badillo, L., Sigala, J., … Neri-Castro, E. (2025). Venom variation and ontogenetic changes in the Crotalus molossus complex: Insights into composition, activities, and antivenom neutralization. *Comparative Biochemistry and Physiology Part C: Toxicology & Pharmacology*, *290*, 110129. https://doi.org/10.1016/j.cbpc.2025.110129

Camacho, E., Escalante, T., Remans, K., Gutiérrez, J. M., & Rucavado, A. (2019). Site mutation of residues in a loop surrounding the active site of a P I snake venom metalloproteinase abrogates its hemorrhagic activity. *Biochemical and Biophysical Research Communications*, *512*(4), 859–863. https://doi.org/10.1016/j.bbrc.2019.03.152

Castro-Amorim, J., Novo de Oliveira, A., Da Silva, S. L., Soares, A. M., Mukherjee, A. K., Ramos, M. J., & Fernandes, P. A. (2023). Catalytically Active Snake Venom PLA2 Enzymes: An Overview of Its Elusive Mechanisms of Reaction. *Journal of Medicinal Chemistry*, *66*(8), 5364–5376. https://doi.org/10.1021/acs.jmedchem.3c00097

Chang, J., Blazek, E., & Carlson, R. P. (1987). Inhibition of phospholipase A2 (PLA2) activity by nifedipine and nisoldipine is independent of their calcium-channel-blocking activity. *Inflammation*, *11*(3), 353–364. https://doi.org/10.1007/BF00915839

Chen, Y.-H., Wang, Y.-M., Hseu, M.-J., & Tsai, I.-H. (2004). Molecular evolution and structure–function relationships of crotoxin-like and asparagine-6-containing phospholipases A2 in pit viper venoms. *Biochemical Journal*, *381*(1), 25–34. https://doi.org/10.1042/BJ20040125

Chowdhury, A., Fry, B. G., Samuel, S. P., Bhalla, A., Vaiyapuri, S., Bhargava, P., Carter, R. W., & Lewin, M. R. (2024). In vitro anticoagulant effects of Bungarus venoms on human plasma which are effectively neutralized by the PLA2-inhibitor varespladib. *Toxicon*, *252*, 108178. https://doi.org/10.1016/j.toxicon.2024.108178

Colis-Torres, A., Neri-Castro, E., Strickland, J. L., Olvera-Rodríguez, A., Borja, M., Calvete, J., Jones, J., Parkinson, C. L., Bañuelos, J., López De León, J., & Alagón, A. (2022). Intraspecific venom variation of Mexican West Coast Rattlesnakes (Crotalus basiliscus) and its implications for antivenom production. *Biochimie*, *192*, 111–124. https://doi.org/10.1016/j.biochi.2021.10.006

Çomaklı, S., Küçükler, S., Değirmençay, Ş., Bolat, İ., & Özdemir, S. (2024). Quinacrine, a PLA2 inhibitor, alleviates LPS-induced acute kidney injury in rats: Involvement of TLR4/NF-κB/TNF α-mediated signaling. *International Immunopharmacology*, *126*, 111264. https://doi.org/10.1016/j.intimp.2023.111264

Cotrim, C. A., De Oliveira, S. C. B., Diz Filho, E. B. S., Fonseca, F. V., Baldissera, L., Antunes, E., Ximenes, R. M., Monteiro, H. S. A., Rabello, M. M., Hernandes, M. Z., De Oliveira Toyama, D., & Toyama, M. H. (2011). Quercetin as an inhibitor of snake venom secretory phospholipase A2. *Chemico-Biological Interactions*, *189*(1–2), 9–16. https://doi.org/10.1016/j.cbi.2010.10.016

Crosland, R. D. (1989). Effect of chlorpromazine and quinacrine on the lethality in mice of the venoms and neurotoxins from several snakes. *Toxicon*, *27*(6), 655–663. https://doi.org/10.1016/0041-0101(89)90016-0

Dahlbäck, B. (2000). Blood coagulation. *The Lancet*, *355*(9215), 1627–1632. https://doi.org/10.1016/S0140-6736(00)02225-X

Datta, G., Dong, A., Witt, J., & Tu, A. T. (1995). Biochemical characterization of basilase, a fibrinolytic enzyme from Crotalus basiliscus basiliscus. *Archives of Biochemistry and Biophysics*, *317*(2), 365–373. https://doi.org/10.1006/abbi.1995.1176

Dennis, E. A., Cao, J., Hsu, Y.-H., Magrioti, V., & Kokotos, G. (2011). Phospholipase A2 enzymes: Physical structure, biological function, disease implication, chemical inhibition, and therapeutic intervention. *Chemical Reviews*, *111*(10), 6130–6185. https://doi.org/10.1021/cr200085w

Depasse, F., Binder, N. B., Mueller, J., Wissel, T., Schwers, S., Germer, M., Hermes, B., & Turecek, P. L. (2021). Thrombin generation assays are versatile tools in blood coagulation analysis: A review of technical features, and applications from research to laboratory routine. *Journal of Thrombosis and Haemostasis*, *19*(12), 2907–2917. https://doi.org/10.1111/jth.15529

Dollingers, P. (2025, July 27). Basilisken-Klapperschlange. *Zootier-Lexikon*. https://www.zootier-lexikon.org/kriechtiere-reptilia/schlangen/grubenottern/basilisken-klapperschlange-crotalus-basiliscus

Escalante, T., Rucavado, A., Fox, J. W., & Gutiérrez, J. M. (2011). Key events in microvascular damage induced by snake venom hemorrhagic metalloproteinases. *Journal of Proteomics*, *74*(9), 1781–1794. https://doi.org/10.1016/j.jprot.2011.03.026

Faure, G., Gowda, V. T., & Maroun, R. C. (2007). Characterization of a human coagulation factor Xa-binding site on Viperidae snake venom phospholipases A2 by

affinity binding studies and molecular bioinformatics. *BMC Structural Biology*, *7*(1), 82. https://doi.org/10.1186/1472-6807-7-82

Fox, J. W., & Serrano, S. M. T. (2008). Insights into and speculations about snake venom metalloproteinase (SVMP) synthesis, folding and disulfide bond formation and their contribution to venom complexity. *The FEBS Journal*, *275*(12), 3016–3030. https://doi.org/10.1111/j.1742-4658.2008.06466.x

Freyssinet, J. M., Gauchy, J., & Cazenave, J. P. (1986). The effect of phospholipids on the activation of protein C by the human thrombin-thrombomodulin complex. *The Biochemical Journal*, *238*(1), 151–157. https://doi.org/10.1042/bj2380151

Ganrot, P. O., & Scherstén, B. (1967). Serum α2-macroglobulin concentration and its variation with age and sex. *Clinica Chimica Acta*, *15*(1), 113–120. https://doi.org/10.1016/0009-8981(67)90333-6

Gimenez, B. T., Cezarette, G. N., Bomfim, A. de S., Monteiro, W. M., Russo, E. M. de S., Frantz, F. G., Sampaio, S. V., & Sartim, M. A. (2020). Role of crotoxin in coagulation: Novel insights into anticoagulant mechanisms and impairment of inflammation-induced coagulation. *The Journal of Venomous Animals and Toxins Including Tropical Diseases*, *26*, e20200076. https://doi.org/10.1590/1678-9199-JVATITD-2020-0076

Gouet, P., Courcelle, E., Stuart, D. I., & M√©toz, F. (1999). ESPript: Analysis of multiple sequence alignments in PostScript. *Bioinformatics*, *15*(4), 305–308. https://doi.org/10.1093/bioinformatics/15.4.305

Gutierres, P. G., Pereira, D. R., Vieira, N. L., Arantes, L. F., Silva, N. J., Torres-Bonilla, K. A., Hyslop, S., Morais-Zani, K., Nogueira, R. M. B., Rowan, E. G., & Floriano, R. S. (2022). Action of Varespladib (LY-315920), a Phospholipase A2 Inhibitor, on the Enzymatic, Coagulant and Haemorrhagic Activities of Lachesis muta rhombeata (South-American Bushmaster) Venom. *Frontiers in Pharmacology*, *12*, 812295. https://doi.org/10.3389/fphar.2021.812295

Hemker, H. C., De Smedt, E., & Al Dieri, R. (2007). The contribution of α_2-macroglobulin thrombin to the endogenous thrombin potential. *British Journal of Haematology*, *139*(3), 513–513. https://doi.org/10.1111/j.1365-2141.2007.06834.x

Ignjatovic, V., Greenway, A., Summerhayes, R., & Monagle, P. (2007). Thrombin generation: The functional role of alpha-2-macroglobulin and influence of developmental haemostasis. *British Journal of Haematology*, *138*(3), 366–368. https://doi.org/10.1111/j.1365-2141.2007.06663.x

Judge, R. K., Henry, P. J., d'Aprile, A. C., Lynch, D., Jelinek, G. A., Wilce, M. C. J., & Wilce, J. A. (2002). Identification of PLA2 and α-Neurotoxin Proteins in the Venom of Pseudonaja affinis (Dugite). *Toxicology and Applied Pharmacology*, *181*(3), 184–191. https://doi.org/10.1006/taap.2002.9416

Kazandjian, T. D., Arrahman, A., Still, K. B. M., Somsen, G. W., Vonk, F. J., Casewell, N. R., Wilkinson, M. C., & Kool, J. (2021). Anticoagulant Activity of Naja nigricollis Venom Is

Mediated by Phospholipase A2 Toxins and Inhibited by Varespladib. *Toxins*, *13*(5), 302. https://doi.org/10.3390/toxins13050302

Kini, R. M. (2005). Structure-function relationships and mechanism of anticoagulant phospholipase A2 enzymes from snake venoms. *Toxicon: Official Journal of the International Society on Toxinology*, *45*(8), 1147–1161. https://doi.org/10.1016/j.toxicon.2005.02.018

Kini, R. M., & Evans, H. J. (1987). Structure-function relationships of phospholipases. The anticoagulant region of phospholipases A2. *The Journal of Biological Chemistry*, *262*(30), 14402–14407.

Kini, R. M., & Iwanaga, S. (1986). Structure-function relationships of phospholipases I: Prediction of presynaptic neurotoxicity. *Toxicon*, *24*(6), 527–541. https://doi.org/10.1016/0041-0101(86)90173-x

Lagrange, J., Lecompte, T., Knopp, T., Lacolley, P., & Regnault, V. (2022). Alpha-2-macroglobulin in hemostasis and thrombosis: An underestimated old double-edged sword. *Journal of Thrombosis and Haemostasis*, *20*(4), 806–815. https://doi.org/10.1111/jth.15647

Lemos-Espinal, J. A., & Smith, G. R. (2020). A checklist of the amphibians and reptiles of Sinaloa, Mexico with a conservation status summary and comparisons with neighboring states. *ZooKeys*, *931*, 85–114. https://doi.org/10.3897/zookeys.931.50922

Lewin, M., Samuel, S., Merkel, J., & Bickler, P. (2016). Varespladib (LY315920) Appears to Be a Potent, Broad-Spectrum, Inhibitor of Snake Venom Phospholipase A2 and a Possible Pre-Referral Treatment for Envenomation. *Toxins*, *8*(9), 248. https://doi.org/10.3390/toxins8090248

Lindahl, M., & Tagesson, C. (1997). FLAVONOIDS AS PHOSPHOLIPASE A2 INHIBITORS: Importance of Their Structure for Selective Inhibition of Group II Phospholipase A2. *Inflammation*, *21*(3), 347–356. https://doi.org/10.1023/A:1027306118026

Mackessy, S. P. (2010). Evolutionary trends in venom composition in the Western Rattlesnakes (Crotalus viridis sensu lato): Toxicity vs. tenderizers. *Toxicon*, *55*(8), 1463–1474. https://doi.org/10.1016/j.toxicon.2010.02.028

Manjunatha Kini, R., & Iwanaga, S. (1986). Structure - function relationships of phospholipases II: Charge density distribution and the myotoxicity of presynaptically neurotoxic phospholipases. *Toxicon*, *24*(9), 895–905. https://doi.org/10.1016/0041-0101(86)90090-5

McCranie, J. R. (1981). *Crotalus basiliscus*. http://hdl.handle.net/2152/45202

Méndez-Molina, R., Villela-Oriza, A. K., Espinosa-Couoh, A. A., & Huchim-Lara, O. (2024). Snakebites epidemiology in Mexico: A 13-year ecological analysis. *Transactions of The Royal Society of Tropical Medicine and Hygiene*, *118*(2), 118–126. https://doi.org/10.1093/trstmh/trad070

Meyer, S., Hartmann, F., Stein, P., Lenherr, R., Fuchs, J., & Spahn, D. R. (2017). Massive coagulopathy caused by the bite of a Crotalus basiliscus snake. *Anaesthesia Cases*, *5*(1), 60–65. https://doi.org/10.21466/ac.FCOABBC.2017

Mounier, C., Franken, P. A., Verheij, H. M., & Bon, C. (1996). The Anticoagulant Effect of the Human Secretory Phospholipase A_2 on Blood Plasma and on a Cell-Free System is Due to a Phospholipid-Independent Mechanism of Action Involving the Inhibition of Factor Va. *European Journal of Biochemistry*, *237*(3), 778–785. https://doi.org/10.1111/j.1432-1033.1996.0778p.x

Mounier, C. M., Bon, C., & Kini, R. M. (2001). Anticoagulant Venom and Mammalian Secreted Phospholipases A_2: Protein- versus Phospholipid-Dependent Mechanism of Action. *Pathophysiology of Haemostasis and Thrombosis*, *31*(3–6), 279–287. https://doi.org/10.1159/000048074

Mukherjee, A. K., Doley, R., & Saikia, D. (2008). Isolation of a snake venom phospholipase A2 (PLA2) inhibitor (AIPLAI) from leaves of Azadirachta indica (Neem): Mechanism of PLA2 inhibition by AIPLAI in vitro condition. *Toxicon*, *51*(8), 1548–1553. https://doi.org/10.1016/j.toxicon.2008.03.021

Mustonen, P., Lehtonen, J. Y. A., & Kinnunen, P. K. J. (1998). Binding of Quinacrine to Acidic Phospholipids and Pancreatic Phospholipase A2. Effects on the Catalytic Activity of the Enzyme. *Biochemistry*, *37*(35), 12051–12057. https://doi.org/10.1021/bi980430q

Myers, P., Espinosa, R., Parr, C. S., Jones, T., Hammond, G. S., & Dewey, T. A. (2025). Crotalus. *The Animal Diversity Web*. https://animaldiversity.org/accounts/Crotalus/classification/

National Center for Biotechnology Information. (2025a). *PubChem Compound Summary for CID 237, (+-)-Quinacrine*. https://pubchem.ncbi.nlm.nih.gov/compound/Quinacrine

National Center for Biotechnology Information. (2025b). *PubChem Compound Summary for CID 4485, Nifedipine*. https://pubchem.ncbi.nlm.nih.gov/compound/Nifedipine

National Center for Biotechnology Information. (2025c). *PubChem Compound Summary for CID 4499, Nisoldipine*. https://pubchem.ncbi.nlm.nih.gov/compound/Nisoldipine

National Center for Biotechnology Information. (2025d). *PubChem Compound Summary for CID 155815, Varespladib*. https://pubchem.ncbi.nlm.nih.gov/compound/Varespladib

National Center for Biotechnology Information. (2025e). *PubChem Compound Summary for CID 5280343, Quercetin*. https://pubchem.ncbi.nlm.nih.gov/compound/Quercetin

National Center for Biotechnology Information. (2025f). *PubChem Compound Summary for CID 5280805, Rutin*. https://pubchem.ncbi.nlm.nih.gov/compound/Rutin

Neri Castro, E. E., Bénard-Valle, M., Alagón, A., Gil, G., López De León, J., & Borja, M. (2020). SERPIENTES VENENOSAS EN MÉXICO: UNA REVISIÓN AL ESTUDIO DE LOS VENENOS, LOS ANTIVENENOS Y LA EPIDEMIOLOGÍA. *Revista Latinoamericana de Herpetología*, *3*(2), 5. https://doi.org/10.22201/fc.25942158e.2020.2.205

Olaoba, O. T., Karina Dos Santos, P., Selistre-de-Araujo, H. S., & Ferreira De Souza, D. H. (2020). Snake Venom Metalloproteinases (SVMPs): A structure-function update. *Toxicon: X*, *7*, 100052. https://doi.org/10.1016/j.toxcx.2020.100052

Rijkers, D. T. S., Wielders, S. J. H., Béguin, S., & Hemker, H. C. (1998). Prevention of the Influence of Fibrin and α2-Macroglobulin in the Continuous Measurement of the Thrombin Potential. *Thrombosis Research*, *89*(4), 161–169. https://doi.org/10.1016/S0049-3848(97)00312-5

Saikia, D., & Mukherjee, A. K. (2017). Anticoagulant and Membrane Damaging Properties of Snake Venom Phospholipase A2 Enzymes. In H. Inagaki, C.-W. Vogel, A. K. Mukherjee, & T. R. Rahmy (Eds.), *Snake Venoms* (pp. 87–104). Springer Netherlands. https://doi.org/10.1007/978-94-007-6410-1_18

Sales, T., Marcussi, S., Da Cunha, E., Kuca, K., & Ramalho, T. (2017). Can Inhibitors of Snake Venom Phospholipases A2 Lead to New Insights into Anti-Inflammatory Therapy in Humans? A Theoretical Study. *Toxins*, *9*(11), 341. https://doi.org/10.3390/toxins9110341

Salvador, G. H. M., Borges, R. J., Lomonte, B., Lewin, M. R., & Fontes, M. R. M. (2021). The synthetic varespladib molecule is a multi-functional inhibitor for PLA2 and PLA2-like ophidic toxins. *Biochimica et Biophysica Acta (BBA) - General Subjects*, *1865*(7), 129913. https://doi.org/10.1016/j.bbagen.2021.129913

Salvador, G. H. M., Gomes, A. A. S., Bryan-Quirós, W., Fernández, J., Lewin, M. R., Gutiérrez, J. M., Lomonte, B., & Fontes, M. R. M. (2019). Structural basis for phospholipase A2-like toxin inhibition by the synthetic compound Varespladib (LY315920). *Scientific Reports*, *9*(1), 17203. https://doi.org/10.1038/s41598-019-53755-5

Sanchez, J. (2024, September 10). Population density in Mexico in 2020, by federal entity. *Statista*. https://www.statista.com/statistics/1323129/mexico-population-density-by-state/

Sánchez, M., Solano, G., Vargas, M., Reta-Mares, F., Neri-Castro, É., Alagón, A., Sánchez, A., Villalta, M., León, G., & Segura, Á. (2020). Toxicological profile of medically relevant Crotalus species from Mexico and their neutralization by a Crotalus basiliscus/Bothrops asper antivenom. *Toxicon*, *179*, 92–100. https://doi.org/10.1016/j.toxicon.2020.03.006

Segura, Á., Herrera, M., Reta Mares, F., Jaime, C., Sánchez, A., Vargas, M., Villalta, M., Gómez, A., Gutiérrez, J. M., & León, G. (2017). Proteomic, toxicological and immunogenic characterization of Mexican west-coast rattlesnake (Crotalus basiliscus) venom and its immunological relatedness with the venom of Central American rattlesnake (Crotalus simus). *Journal of Proteomics*, *158*, 62–72. https://doi.org/10.1016/j.jprot.2017.02.015

Shimizu, T., Hansson, G. C., & Strandvik, B. (1994). Effects of Pancreatic and Snake Venom Phospholipase A2 on the Generation of Leukotriene B4 and C4 by Human Leukocytes in Vitro: *Pancreas*, *9*(1), 37–41. https://doi.org/10.1097/00006676-199401000-00005

Sigma-Aldrich. (1997, May 21). *Enzymatic Assay of PHOSPHOLIPASE A2 (EC 3.1.1.4)*. https://www.sigmaaldrich.com/deepweb/assets/sigmaaldrich/marketing/global/documents/400/286/phospholipa21.pdf?srsltid=AfmBOooSjVp07jFfz6Y_p_slyL8z8dFu8xWqHSCTCVRgsBYsZIUG05L8

Stefansson, S., Kini, R. M., & Evans, H. J. (1990). The basic phospholipase A2 from Naja nigricollis venom inhibits the prothrombinase complex by a novel nonenzymic mechanism. *Biochemistry*, *29*(33), 7742–7746. https://doi.org/10.1021/bi00485a024

Svoboda, P., Meier, J., & Freyvogel, T. A. (1995). Purification and characterization of three α2-antiplasmin and α2-macroglobulin inactivating enzymes from the venom of the Mexican west coast rattlesnake (Crotalus basiliscus). *Toxicon*, *33*(10), 1331–1346. https://doi.org/10.1016/0041-0101(95)00065-T

The UniProt Consortium, Bateman, A., Martin, M.-J., Orchard, S., Magrane, M., Adesina, A., Ahmad, S., Bowler-Barnett, E. H., Bye-A-Jee, H., Carpentier, D., Denny, P., Fan, J., Garmiri, P., Gonzales, L. J. D. C., Hussein, A., Ignatchenko, A., Insana, G., Ishtiaq, R., Joshi, V., … Zhang, J. (2025). UniProt: The Universal Protein Knowledgebase in 2025. *Nucleic Acids Research*, *53*(D1), D609–D617. https://doi.org/10.1093/nar/gkae1010

Tunstall, A. M., Merriman, J. M., Milne, I., & James, K. (1975). Normal and pathological serum levels of alpha2-macroglobulins in men and mice. *Journal of Clinical Pathology*, *28*(2), 133–139. https://doi.org/10.1136/jcp.28.2.133

Uetz, P. (n.d.). Crotalus basiliscus (COPE, 1864). *The Reptile Database*. Retrieved June 30, 2025, from https://reptile-database.reptarium.cz/species?genus=Crotalus&species=basiliscus

Verheij, H. M., Boffa, M. C., Rothen, C., Bryckaert, M. C., Verger, R., & de Haas, G. H. (1980). Correlation of enzymatic activity and anticoagulant properties of phospholipase A2. *European Journal of Biochemistry*, *112*(1), 25–32. https://doi.org/10.1111/j.1432-1033.1980.tb04982.x

Yoshino, S., Fujimoto, K., Takada, T., Kawamura, S., Ogawa, J., Kamata, Y., Kodera, Y., & Shichiri, M. (2019). Molecular form and concentration of serum α2-macroglobulin in diabetes. *Scientific Reports*, *9*(1), 12927. https://doi.org/10.1038/s41598-019-49144-7

13 Tables and Figures

Tables

Figures

14 Appendix

14.1 Anion Exchange Chromatography – a2M-inhibiting Proteases

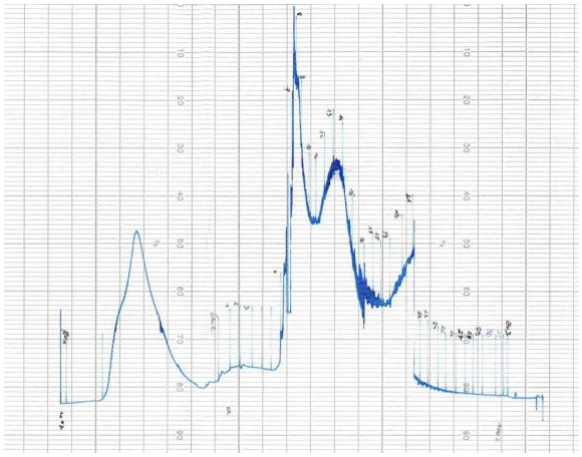

This scanned chromatogram corresponds to the AEC in Figure 3.

14.2 Size Exclusion Chromatography – a2M-inhibiting Proteases

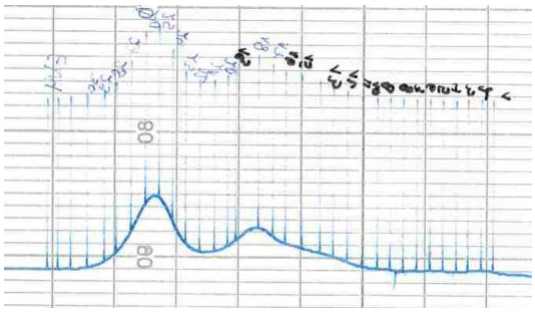

This scanned chromatogram corresponds to the SEC in Figure 4.

14.3 Size exclusion chromatography – Phospholipase A2

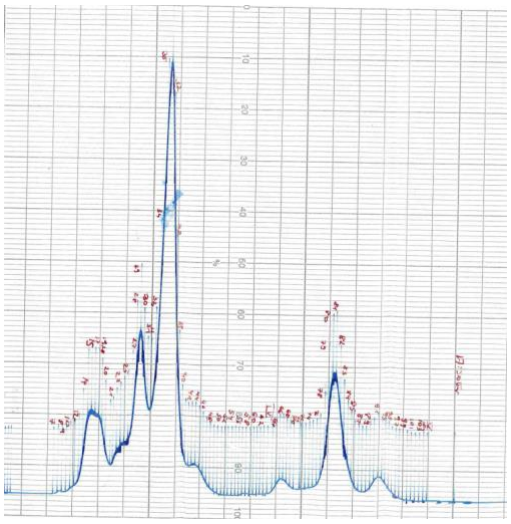

This scanned chromatogram corresponds to the SEC in Figure 12.

14.4 Anion Exchange Chromatography 1– Phospholipase A2

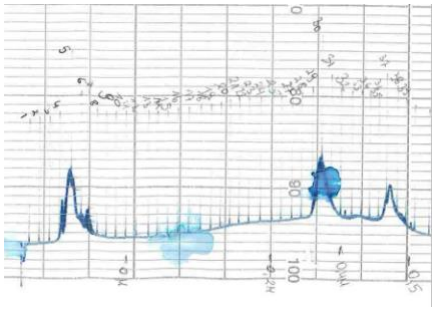

This scanned chromatogram corresponds to the AEC1 in Figure 13.

14.5 Anion Exchange Chromatography 2– Phospholipase A2

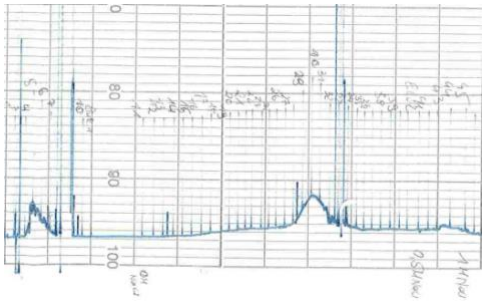

This scanned chromatogram corresponds to the AEC2 in Figure 14.